Accepted Manuscript

Design, synthesis, biological evaluation, molecular docking and QSAR studies of 2,4-dimethylacridones as anticancer agents

Manikanta Murahari, Prashant S. Kharkar, Nitin Lonikar, C. Yergeri Mayur

PII: S0223-5234(17)30087-9

DOI: 10.1016/j.ejmech.2017.02.022

Reference: EJMECH 9218

To appear in: *European Journal of Medicinal Chemistry*

Received Date: 7 January 2017

Revised Date: 7 February 2017

Accepted Date: 8 February 2017

Please cite this article as: M. Murahari, P.S. Kharkar, N. Lonikar, C.Y. Mayur, Design, synthesis, biological evaluation, molecular docking and QSAR studies of 2,4-dimethylacridones as anticancer agents, *European Journal of Medicinal Chemistry* (2017), doi: 10.1016/j.ejmech.2017.02.022.

Design, synthesis, biological evaluation, molecular docking and QSAR studies of 2,4-Dimethylacridones as anticancer agents

Manikanta Murahari[a,b], Prashant S. Kharkar[c], Nitin Lonikar[d], Mayur C. Yergeri[c]*

[a]Department of Pharmaceutical Chemistry, SVKM's Dr. Bhanuben Nanavati College of Pharmacy, Mumbai-400 056. India.

[b]Department of Pharmaceutical Chemistry, Faculty of Pharmacy, M.S. Ramaiah University of Applied Sciences, Bangalore-560 054, India.

[c]Department of Pharmaceutical Chemistry, SPP School of Pharmacy & Technology Management, SVKM's NMIMS, Mumbai-400 056. India.

[d]Department of Pharmaceutical Chemistry, AME's V.L. College of Pharmacy, Raichur-584103. India

Graphical Abstract

Multidrug resistance in cancer is an unmet challenge and drawback for the failure of many chemotherapeutic drugs. Search for targeted, effective drug with minimum toxicity is an urgent need. An attempt has been made to explore the chemosensitizing ability of 2,4-dimethylacridones with alkyl side chain containing substituting tertiary amines at the end of the side chain. Considering the structural features required for the MDR reversal activity, 2,4-dimethylacridone with propyl and butyl side chain containing various tertiary amino groups like morpholinyl, piperidinyl, N-methyl piperazinyl, N,N-diethylamino, N-diethanolamino, β-hydroxylethyl piperazino at the terminus of the alkyl side chain have been synthesized, characterized and screened for anticancer and MDR modulation activity.

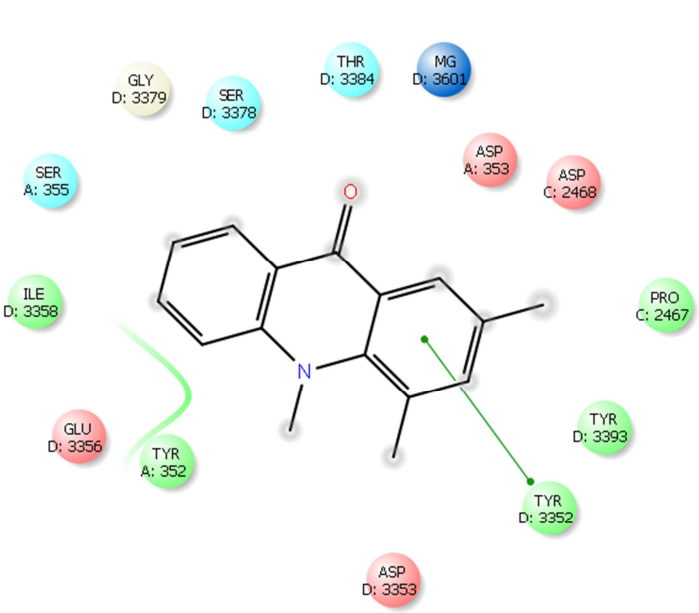

The 2D interaction diagram of compound **10** with P-gp

Cytotoxicity profile of active compounds

Compound Code	IC_{50} (µM) ± SD MCF7	IC_{50} (µM) ± SD MCF7/ADR	Vinblastine IC_{50} (nM) ± SD MCF7/ADR	Fold potentiation
12e	4 ± 0.05	5.21 ± 0.13	3.11 ± 0.06	Complete
12f	2 ± 0.03	2.56 ± 0.05	1.25 ± 0.05	Complete

Design, synthesis, biological evaluation, molecular docking and QSAR studies of 2,4-Dimethylacridones as anticancer agents

Manikanta Murahari[a,b], Prashant S. Kharkar[c], Nitin Lonikar[d], Mayur YC[c]*

[a]Department of Pharmaceutical Chemistry, SVKM's Dr. Bhanuben Nanavati College of Pharmacy, Mumbai-400 056. India.

[b]Department of Pharmaceutical Chemistry, Faculty of Pharmacy, Ramaiah University of Applied Sciences, Bangalore-560 054, India.

[c]Department of Pharmaceutical Chemistry, SPP School of Pharmacy & Technology Management, SVKM's NMIMS, Mumbai-400 056. India.

[d]Department of Pharmaceutical Chemistry, AME's V.L. College of Pharmacy, Raichur-584103. India

*Corresponding Author:

Dr. Mayur C. Yergeri

Department of Pharmaceutical Chemistry,
SPPSPTM
SVKM's NMIMS University
Vile Parle (West), Mumbai- 400 056. India.
Tel: (+91)- 9930713869,
Fax: 0091-22-26132905
E-mail: mayuryc@rediff.com, mayuryc@hotmail.com

Abstract:

Drug resistance in cancer is an unmet medical challenge and a major drawback for the failure of many chemotherapeutic drugs. Search for targeted, effective drug with minimum toxicity is an urgent need. Acridone which is an alkaloid derivative has been attributed as molecule in reversing drug resistance in cancer cells for a long time now. In the present investigation, an attempt has been made to explore the chemosensitizing ability of 2,4-dimethylacridones with alkyl side chain containing terminally substituted tertiary amino groups. Considering the structural features required for the MDR reversal activity, acridone derivatives have been synthesized with propyl and butyl side chain containing morpholinyl, piperidinyl, *N*-methylpiperazinyl, *N*,*N*-diethylamino, *N*-diethanolamino, *N*-[(β-hydroxylethyl)]piperazino at the terminus of the alkyl side chain. cLogP values for the synthesized compounds ranged from 2.96 to 4.72 for the propyl derivatives and 3.41 to 5.15 for the butyl derivatives. All the compounds were screened against breast cancer sensitive MCF7 and resistant MCF7/ADR cell lines. Compounds **12e** and **12f** have shown better cytotoxicity profiles with IC_{50} of 4 ± 0.05 and 2 ± 0.03 µM against MCF7 cells, 5.21 ± 0.13 and 2.56 ± 0.05 µM against MCF7/ADR cells. Photolabeling studies with [^{3}H]-azidopine and molecular docking studies have identified that 2,4-dimethylacridones have potential to modulate the P-gp mediated multidrug resistance. Docking studies identified that compounds have shown favorable interactions with P-gp. QSAR equation was derived for cytotoxicity *vs* molecular descriptors of acridone derivatives. Best models with good predictive ability have been generated with very high square correlation coefficient (R^2) values of 0.889, 0.964 and 0.983.

Keywords: Acridones, Chemosensitizers, Drug Resistance, Phase Transfer Catalysis (PTC), Molecular Docking

1. Introduction:

The major goal of oncology scientists is to design an effective anticancer agent which is not only sensitive in normal cancer cells but also against drug resistant cancers. In principle, drug resistance in cancer treatment has remained as an impediment to successful chemotherapy. Thirty years of research in cancer and its multidrug resistance has identified a myriad of mechanism in which tumor cells efflux chemotherapeutic agents. Chemotherapy is baffling the cancer scientists all over the world, and it has become evident that resistance exists against every

effective anticancer drug including the recently introduced drugs [1-4]. Therefore, the ability to predict and alter or block the drug resistance mechanism in cancer is likely to improve the therapeutic index. Acquired drug resistance has become common due to the overexpression of one or more energy-dependent transporters P-gylcoprotein/ABCB1 that eject anticancer agents out of cells, which contribute to the failure of chemotherapy. Another important factor is delivery of anticancer drug to the target tissue which may vary from patient to patient. Penetration of the drug into tumor cells protected by different mechanisms like altered pH or tumor vasculature, increased hydrostatic pressure is a major task. Potential reasons for the failure of these drugs against cancer are attributed due to low affinity, poor specificity and low bioavailability at the tumor site [5-7].

Acronycine a natural alkaloid was isolated from the bark of *Acronychia baurri* in 1948 [8]. Acronycine has shown promising activity against wide spectrum of cancers in lab animals. Glyfoline, alkaloid from *Glycosmis citrifolia* was found to be potent molecule with an IC_{50} of 2.2 µM in HL60 cells [9]. Tricyclic heterocyclic system, acridone has shown interesting applications in the area of cancer by multi-targeting mechanisms, antimalarial, drugs acting on CNS with well identified mechanism and still being explored as an active pharmacophore for various activities [10-15].

Several targets such as DNA toposiomerases and Protein Kinase C (PKC) which play vital roles for the normal functioning of cells such as signal transduction, regulatory mechanisms, etc., have been tried for intervening the tumor progression and metastasis [16]. Of the several classes of anticancer agents, acridones are an interesting class. Numerous research groups have been working on the medicinal chemistry and the biological aspects of acridones as chemotherapeutic agents due to their unique properties. Literature reveals that the acridone alkaloids and their synthetic derivatives possess a wide range of biological activities like anticancer, MDR modulators, etc [17]. The acridone derivatives under clinical development are amsacrine (**1**), anilinoacridine derivative asulacrine (or CI-921) (**2**), *N*-[(2-dimethylamino)ethyl]acridine-4-carboxamide (DACA) (**3**), triazoloacridones (C_{1305} **4** and C_{1533} **5**) and imidazoacridones (C_{1311} **6**) (**Figure 1**) [18]. Literature shows that substitution on 2nd and 4th position in acridone ring show good cytotoxicity [19]. Based on this developments, substitution of methyl groups at the 2nd and 4th positions of the acridone ring has been carried out and this may result in the increased

lipophilicity, which may improve the binding affinity of acridone based derivatives to ABCB1 in reversing drug resistance. Previously, the author's research group has reported the synthesis and screening methods of various acridone derivatives as drug resistant modulators [19].

Several studies have identified that the drug efflux pump P-gp is one of the responsible factors for promoting multidrug resistance in tumor cells and also for altering the pharmacokinetic properties of the drugs [20]. ABCB1 belongs to the superfamily of ATP-binding cassette (ABC) transporters which is encoded by the *MDR1* gene. The protein contains 1280 amino acids arranged in two homologous halves of 610 amino acids joined together by linker of 60 amino acids chain, each half with six transmembrane sequences followed by the nucleotide-binding domain. The exact mechanism of action and its selectivity towards efflux of drugs have not been identified yet. X-ray crystallography studies have identified that the protein has large flexible binding cavity within the domain [21]. A lot of experiments have been carried out on these aspects a new direction has been given to the study of acridones and cancer cytotoxicity and drug resistance mechanism by the author since two decades [19].

Previously the author's group performed molecular docking studies of chloroacridone derivatives against calmodulin-dependent cAMP phosphodiesterase to identify the possible binding interactions. Calmodulin plays vital role in regulating protein kinase activity and other cellular processes. Studies identified that intracellular calcium concentration was greater in resistant cells than non-resistant cells. Also calmodulin inhibitors play significant role by interfering cellular drug accumulation [22]. In the present investigation, authors have designed 2,4-dimethylacridones to evaluate MDR reversal activity against cancer sensitive and resistant cell lines. A lot of data has been accumulated only after the establishment of ABCB1 structure. As of now, not much literature exists about the binding domain with acridones and ABCB1. The authors have tried to compare the same and how the acridone structural modification has proven to give more cytotoxic drugs and also in reversing drug resistance in tumor cells.

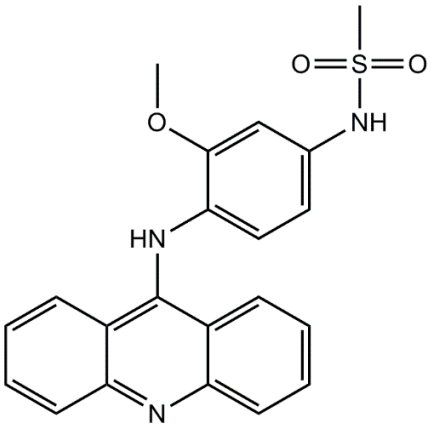

Amsacrine (**1**)

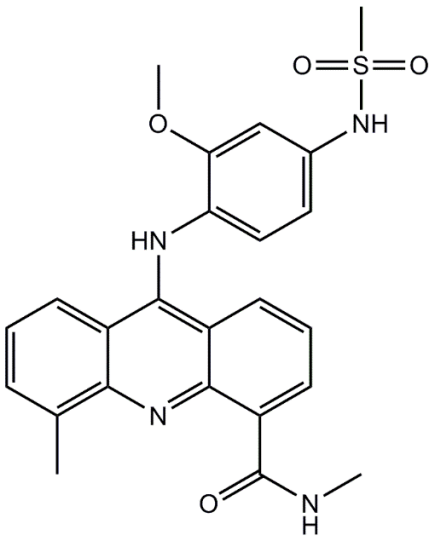

Asulacrine (**2**)

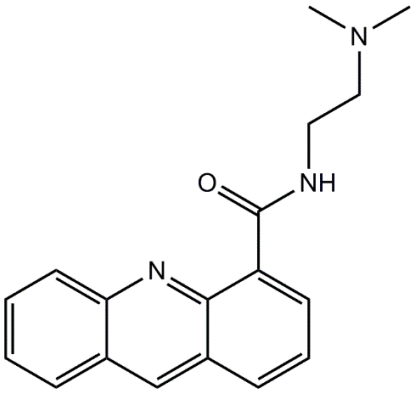

DACA (**3**)

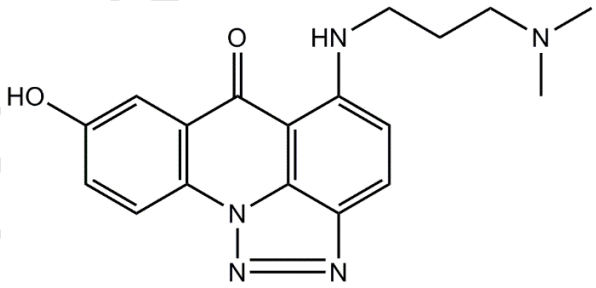

C_{1305} (**4**)

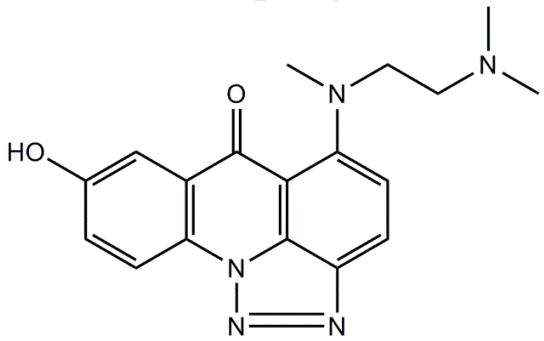

C_{1533} (**5**)

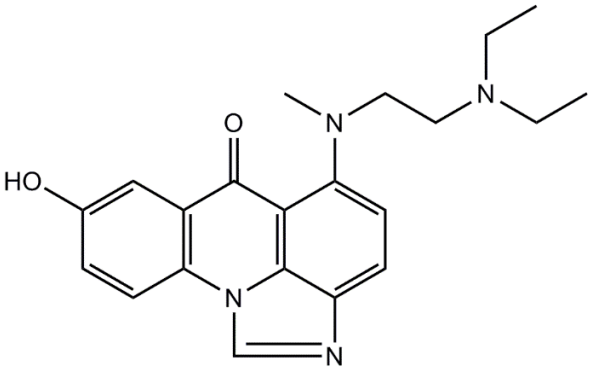

C_{1311} (**6**)

Figure 1. Molecular structures of acridone derivatives under clinical development

2. Results & Discussion:

2.1 Chemistry:

2,4-Dimethylacridone derivatives were synthesized as per general method outlined in **Scheme 1**. The synthesis of title compounds begins with Ullmann condensation of 2-halobenzoic acid (**7**) and 2,4-dimethylaniline (**8**) to form 2-[(2,4-dimethylpheny)amino]benzoic acid (**9**). The starting materials were added in round bottomed flask, mixed well in isoamyl alcohol and refluxed in the presence of copper powder and anhydrous potassium carbonate. Compound **9** was further cyclized with polyphosphoric acid where 2,4-dimethylacridone (**10**) was obtained in high yield (86-90 %). *N*-alkylation i.e., propyl and butyl side chain was attached to compound 10 by the principle of Phase Transfer Catalysis (PTC) in good yields. Later nucleophilic substitution of *N*-alkylated acridones i.e., N^{10}-chloropropyl and N^{10}-chlorobutyl 2,4-dimethylacridone with difference secondary amines was performed in anhydrous potassium carbonate.

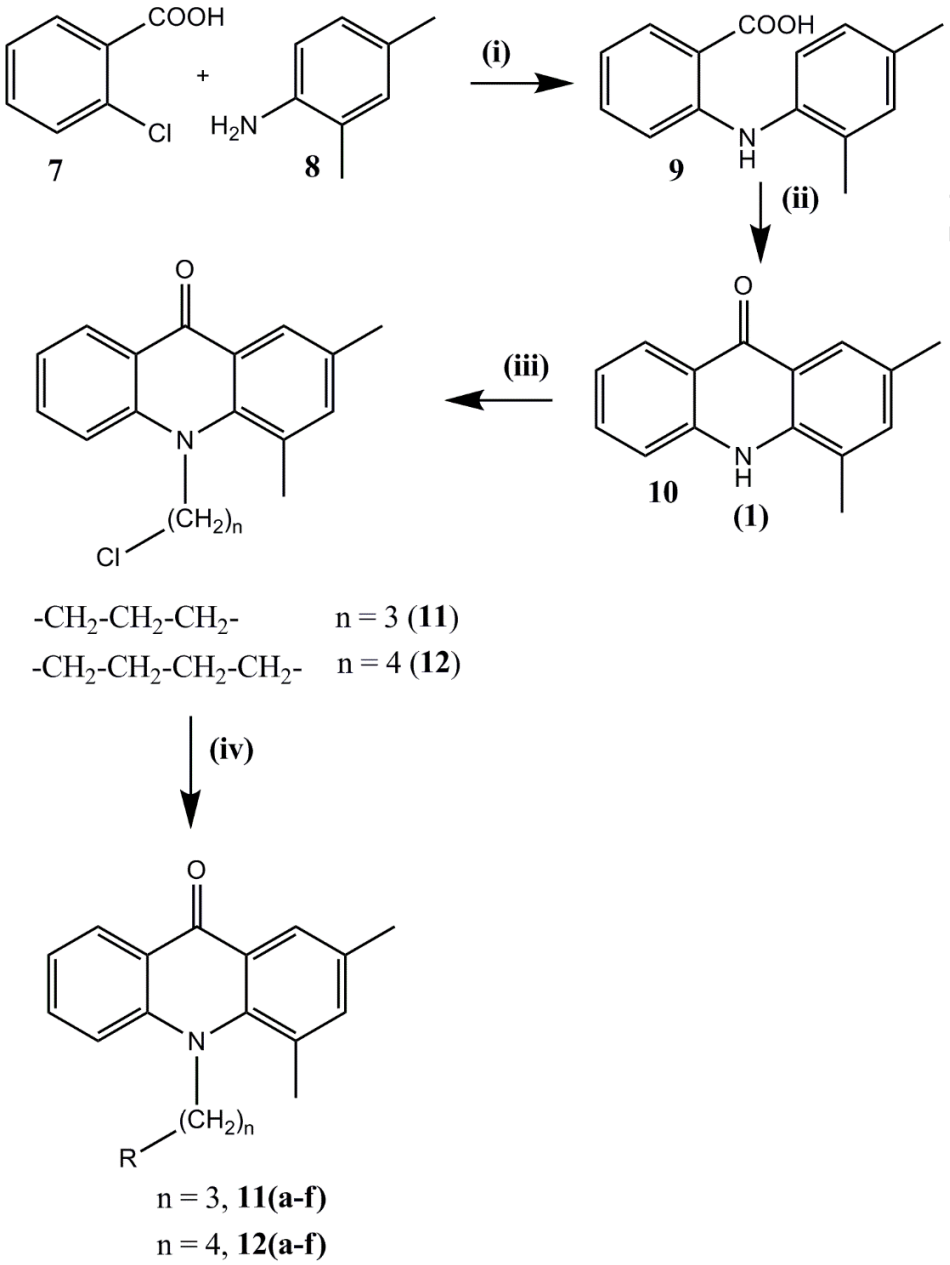

Reagents & Conditions: (i) K_2CO_3, Cu, isoamyl alcohol, reflux, 6h; (ii) PPA, 100 ^{0}C, 3h; (iii) 6N KOH, 1-bromo-3-chloropropane/1-bromo-4-chlorobutane, PTC, RT, 24h; (iv) K_2CO_3, KI, R-H, reflux, 6h.

Scheme 1: Synthesis of 2,4-dimethylacridone derivatives

N-alkylation of acridone can be performed in strictly anhydrous conditions in the presence of strong bases like $NaNH_2$ or NaH because of weakly basic nature of ring nitrogen. The reaction of acridone (**10**) in anhydrous aniline with chlorobromo alkanes in the presence of strong base $NaNH_2$ under reflux yielded respective N^{10}-(chloroalkyl) acridones (**11-12**). However, *N*-alkylation requires vigorous experimental conditions with very low yield. But by the applying the principle of Phase Transfer Catalysis (PTC) compound **10** readily undergoes *N*-alkylation with better yields. *N*-alkylation can be performed at room temperature by stirring acridone derivative and alkylating agent i.e., 1-bromo-3-chloropropane or 1-bromo-4-chlorobutane in a two phases of tetrahydrofuran and 6N aqueous KOH in the presence of tetrabutylammonium bromide. Previous step yields 10-(3-chloropropyl) (**11**) or 10-(4-chlorobutyl) acridone (**12**) in good yields. Later, iodide-catalysed nucleophilic substitution of intermediates with various secondary amines like morpholine, piperidine, pyrrolidine, *N*-methylpiperazine, *N*,*N*-diethylamine, *N*-diethanolamine and β-hydroxyethyl piperazine by refluxing in anhydrous potassium carbonate in acetonitrile yielding the title compounds (**11a-f** and **12 a-f**) as free bases (**Table 1**).

All the synthesized compounds were purified by column chromatography packed with silica gel and purified compounds were characterized by ^{1}H and ^{13}C NMR and Mass spectral methods (Supplementary Material).

Table 1. Physical data of acridone derivatives

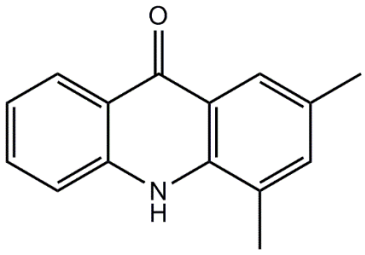

10

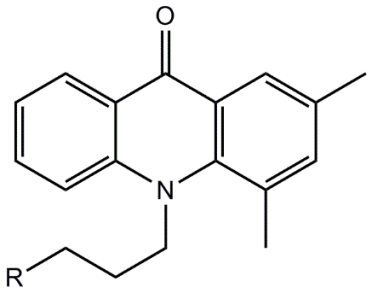

11(a-f)

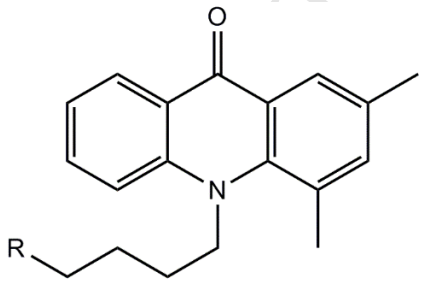

12(a-f)

Compound Code	R	Molecular Formula	Molecular Weight	Melting Point (^{0}C)	Yield %
10	-H	$C_{15}H_{13}NO$	223.27	318	68
11	-Cl	$C_{18}H_{18}ClNO$	299.79	158	46
11a	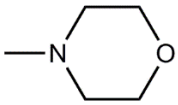	$C_{22}H_{26}N_2O_2$	350.45	159	58
11b	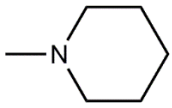	$C_{23}H_{28}N_2O$	348.48	168	33
11c	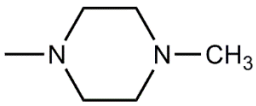	$C_{23}H_{29}N_3O$	363.50	152	59
11d	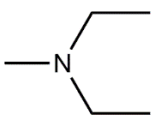	$C_{22}H_{28}N_2O$	336.47	182	42

11e	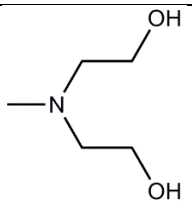	$C_{22}H_{28}N_2O_3$	368.47	193	56
11f	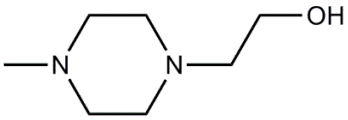	$C_{24}H_{31}N_3O_2$	393.52	223	52
12	-Cl	$C_{19}H_{20}ClNO$	313.82	134	52
12a	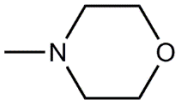	$C_{23}H_{28}N_2O_2$	364.48	148	58
12b	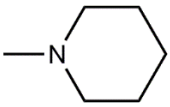	$C_{24}H_{30}N_2O$	362.51	162	53
12c	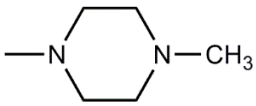	$C_{24}H_{31}N_3O$	377.52	183	59
12d	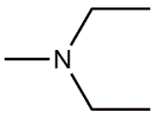	$C_{23}H_{30}N_2O$	350.50	172	58
12e	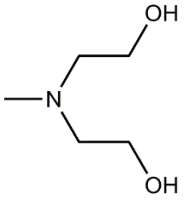	$C_{23}H_{30}N_2O_3$	382.50	142	52
12f	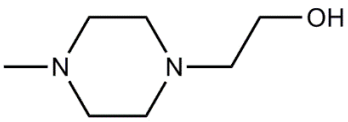	$C_{25}H_{33}N_3O_2$	407.55	181	56

2.2 Biological Activity:

2.2.1 Cytotoxicity studies:

2.2.1.1 *In vitro* cytotoxicity of acridones in human MCF7 and MCF7/ADR cells

Newly synthesized N^{10}-substituted 2,4–dimethylacridone derivatives were screened for *in vitro* anticancer activity in human sensitive MCF7 and resistant MCF-7/ADR cells. Each value represents the mean of recordings in triplicate and results were shown in **Table 2 & Figure 2** and expressed as IC_{50} i.e., concentration required for 50% inhibition of growth of cells treated with respect to cells which are untreated.

Table 2. Cytotoxicity of acridone derivatives on human MCF7 and MCF7/ADR cells and the potentiation of vinblastine cytotoxicity in drug resistant MCF7/ADR cells.

Compound Code	IC_{50} (µM) ± SD[a] MCF7	IC_{50} (µM) ± SD[a] MCF7/ADR	Vinblastine IC_{50} (nM) ± SD[a] MCF7/ADR	Fold Potentiation
10	79 ± 0.12	82.1 ± 0.97	27.12 ± 0.19	1.4
11	ND	ND	ND	ND
11a	59.16 ± 0.22	65.3 ± 0.76	19.9 ± 0.11	6.4
11b	58 ± 0.17	61.7 ± 0.69	17 ± 0.08	7.17
11c	50.21 ± 0.36	53.5 ± 0.43	17.2 ± 0.13	4.75
11d	29.11 ± 0.18	34.2 ± 0.28	14.2 ± 0.08	10.48
11e	19.1 ± 0.09	22.8 ± 0.15	11.22 ± 0.05	9.7
11f	12 ± 0.04	15.1 ± 0.11	8 ± 0.03	16.74
12	ND	ND	ND	ND
12a	20 ± 0.12	21.8 ± 0.19	4 ± 0.03	Complete
12b	30.10 ± 0.19	36.3 ± 0.22	5 ± 0.02	--
12c	14.50 ± 0.09	16.2 ± 0.31	10 ± 0.11	--
12d	8.3 ± 0.03	9.1 ± 0.09	4.05 ± 0.02	Complete

12e	4 ± 0.05	5.21 ± 0.13	3.11 ± 0.06	Complete
12f	2 ± 0.03	2.56 ± 0.05	1.25 ± 0.05	Complete
Vinblastine	3 ± 0.01 nM	69.0 ± 0.2 nM	--	--

Note: At IC_{10} concentration, the modulators were able to reverse drug resistance completely in MCF-7/ADR cancer cells.

ND= Not Determined

a- Results are average of triplicate analysis

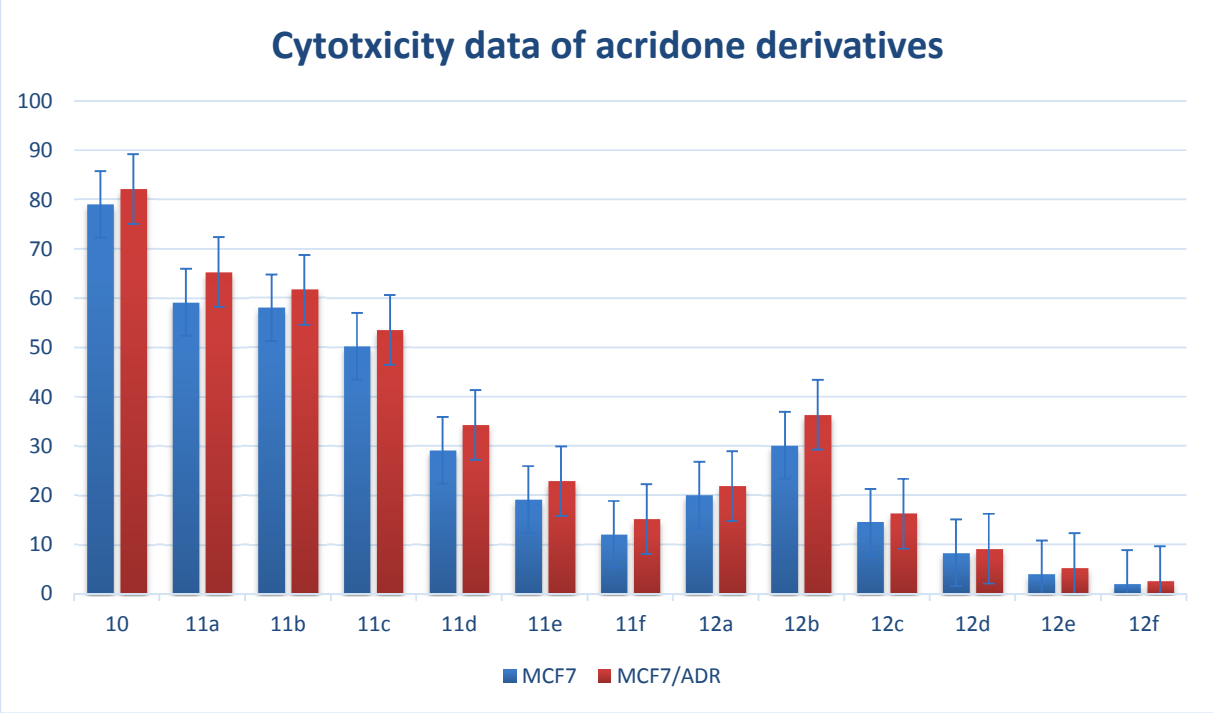

Figure 2. Experimental IC_{50} of acridone derivatives against MCF7 and MCF7/ADR cell lines

Antiproliferative activity of title compounds i.e., N^{10}-2,4-dimethylacridone derivatives were evaluated on human breast adenocarcenoma MCF7 cell line. Results suggests that chemical nature of the secondary amine attached to alkyl side chain of acridone plays a critical role and can be considered as pharmacophoric feature for the cytotoxicity. IC_{50} value of 2,4-dimethylacridone compound **10** is 79 ± 0.12 µM, found least active among the synthesized

compounds indicating that side chain of acridone is essential for cytotoxicity. Considering the tumor physiology, structural features and physicochemical properties like lipophilicity, pKa, acridones with propyl and butyl side chain with terminal secondary amines have been synthesized and screened with an aim of obtaining potent compounds. Title compounds of acridones with propyl side chain *vs* butyl side chain have shown appreciable results and also the study clearly proved that increase in distance from the acridone ring and secondary amine enhanced the anti-proliferative activity and hydrophobicity. Acridones with propyl side chain have shown anticancer activity in the range of IC_{50} (µM) 59.16 ± 0.22 to 12 ± 0.04 and acridones with butyl side chain in the range of 30.10 ± 0.19 to 2 ± 0.03. In the series of acridones with propyl side chain with secondary amines as morpholinyl (**11a**), piperidinyl (**11b**) and *N*-methylpiperazinyl (**11c**) have displayed less cytotoxicity at 59.16 ± 0.22, 58 ± 0.17 and 50.21 ± 0.36. Compound **11d** with secondary amine *N*,*N*-diethylamine and compound **11e** with *N*-diethanolamine have improved the selectivity with cytotoxicity at 29.11 ± 0.18 and 19.1 ± 0.09. Moreover in the series of acridone with propyl side chain series with β-hydroxyethyl piperazine (**11f**) as secondary amine found more favorable with an IC_{50} of 12 ± 0.04. Among the series, acridones containing substituent such as butyl side chain with secondary amines as β-hydroxyethyl piperazine (**12f**), *N*,*N*-diethanolamine (**12e**), *N*,*N*-diethylamine (**12d)** have exerted better cytotoxicity at IC_{50} 2 ± 0.03, 4 ± 0.05, 8.3 ± 0.03 µM respectively (**Table 2**). Similar to the propyl side chain series, compounds with butyl side chain containing secondary amines morpholinyl (**12a**), piperidinyl (**12b**) and *N*-methyl piperazine (**12c**) were found less active against MCF7 with IC_{50} of 20 ± 0.12, 30.10 ± 0.19 and 14.50 ± 0.09. Compound **12f**, acridone containing butyl alkyl side chains with terminal end of β-hydroxyethyl piperazine was found to be potent among the series. Interestingly, hydroxyl group containing secondary amines attached to alkyl side chain of acridones have shown potent and increased the cytotoxicity. These observations revealed that β-hydroxyethyl piperazine as secondary amine is essential for anticancer activity and presence of hydroxyl substituted secondary amines enhance the activity.

The cytotoxicity of 2,4-dimethylacridone derivatives were screened against drug resistant MCF7/ADR cell line to compare the cytotoxicity and the IC_{50} values at micromolar concentration range were presented in **Table 2**. Acridones with secondary amines at the terminal end of propyl side chain have exhibited IC_{50} (µM) in the range of 82.1 ± 0.97 to 15.1 ± 0.11. Similarly acridones with secondary amines and butyl side chain have shown IC_{50} (µM) in the

range of 21.8 ± 0.19 to 2.56 ± 0.05. Also compound **10** have shown less cytotoxicity against MCF7/ADR with an IC_{50} (µM) of 82.1 ± 0.97 indicating that side chain is essential. Furthermore acridones having propyl side chain with secondary amines such as morpholinyl (**11a**), piperidinyl (**11b**) and *N*-methylpiperazinyl (**11c**) have displayed reduced cytotoxicity among the series with an IC_{50} (µM) values of 65.3 ± 0.76, 61.7 ± 0.69, 53.5 ± 0.43 respectively. Comparatively acridones with butyl side chain have shown potential cytotoxicity against both MCF7 and MCF7/ADR cell lines suggesting length of side chain have profound impact. From the study, compounds **12f**, **12e** and **12d** have exhibited good cytotoxicity profile among the derivatives with an IC_{50} (µM) of 2.56 ± 0.05, 5.21 ± 0.13 and 9.1 ± 0.09 respectively. Compound **12f** having β-hydroxyethyl piperazine as secondary amine with butyl side chain have shown significant and highest cytotoxicity against both sensitive and resistant MCF7 and MCF7/ADR cell lines with an IC_{50} (µM) of 2 ± 0.03 and 2.56 ± 0.05. Moreover among the series of acridones with propyl side chain, compound **11f** acridone with β-hydroxyethyl piperazine as secondary amine and propyl side chain have shown good cytotoxicity with IC_{50} (µM) of 15.1 ± 0.11. This highlights the chemical nature of secondary amine plays significant role for cytotoxicity and β-hydroxyethyl piperazine is essential, acridone with β-hydroxyethyl piperazine as secondary amine can be taken as promising hit compound for further design of safe and potent compound.

On the other hand, acridones were found more sensitive to MCF7 rather than drug resistant MCF7/ADR cell line. Multidrug resistance in MCF7/ADR is mediated through many transporters like P-gp or Breast Cancer Resistance Protein (BCRP). Cytotoxicity profile of title compounds against MCF7/ADR indicates that 2,4-dimethylacridones have the ability to inhibit MDR modulation activity mediated through P-gp pump. According to literature, acridones are studied much as P-gp inhibitors and to a lesser extent of other pump inhibitors of MRP family. Also it is reported that acridones exhibit anticancer and anti-MDR activity and is might be through DNA intercalation property [23]. Comparison of IC_{50} values of acridones against MCF7 and MCF7/ADR, clearly identifies that drug resistance in MCF7/ADR cell line is mediated through overexpression of many pumps like P-gp or Breast Cancer Resistance Protein (BCRP) and acridones are not substrates of all the pumps. Interestingly title compounds have shown similar and good cytotoxicity profile against MCF7/ADR cell line, suggesting that 2,4-dimethylacridones might have ability to modulate MDR mediated by P-gp. Furthermore

compounds were screened to identify the ability of title compounds to modulate vinblastine cytotoxicity against MCF7/ADR cell line.

2.2.1.2 Sensitization of drug resistant MCF7 cells by 2,4-dimethylacridones:

In an attempt to discover novel and potent MDR modulators, the 2,4-dimethylacridones were evaluated in drug-resistant cancer cell lines. Aim of the study was to investigate the ability of title compounds to modulate the vinblastine cytotoxicity against MCF-7/ADR cells and to correlate the structure of acridones with MDR reversal activity. Both doxorubicin and vinca alkaloids- vincristine and vinblastine are potent cytotoxic agents and substrates of P-gp [24]. According to Tseng et al., compounds daunomycin and vinblastine have shown IC_{50} values of 7.12 ± 0.42 µM and 0.0106 ±0.004 µM against MCF7/ADR cell line [25]. Photolabelling studies against MCF7/ADR cell line too identified that vinblastine is potent cytotoxic agent and also highly specific to P-gp [26]. Hence, for the sensitization study of acridones against MCF7/ADR cell line we have used highly competitive binding substrate vinblastine. Cells were treated continuously with different concentrations of vinblastine ranging from 0-100 nM for 7 days in the absence or presence of IC_{10} concentration of title compounds as MDR modulators. The IC_{50} value of vinblastine in combination with title compounds against MCF-7/ADR cells was observed in the range of 1.25 ± 0.05 to 27.12 ± 0.19 nM. Each value represents the mean of recordings in triplicate and results were tabulated in **Table 2**.

Multidrug resistance is majorly responsible for the failure of many drugs in the therapy of numerous cancers. Screening of compounds on drug sensitive and resistant cancer cell lines is the fundamental model to evaluate the behavior of compounds, to test the hypothesis and to improve the efficacy [27]. To identify the mechanism and resistance modulating ability, title compounds were screened against cancer sensitive and resistant MCF7 and MCF7/ADR cell lines. Fold potentiation of acridones was calculated with respect to IC_{50} values of MCF7/ADR relative to MCF7 cell line. Comparative study to identify the ability of 2,4-dimethylacridones as MDR modulators in potentiation of cytotoxicity of vinblastine revealed that compounds **12a, 12d, 12e & 12f** demonstrated the greatest effect. *In vitro* data of acridones were summarized in **Table 2**. Both the series of acridone derivatives have shown appreciable results. Interestingly acridones with butyl side chain series have displayed better cytotoxicity profile in resistant cell line MCF7/ADR compared to propyl side chain series, might be because of improved

hydrophobicity. Moreover, acridones containing secondary amines as morpholine (**12a**), *N,N*-diethylamine (**12d**), *N*-diethanolamine (**12e**) and β-hydroxyethyl piperazine (**12f**) were able to completely reverse MDR modulation because of hydrophobicity and basicity. In the absence of 2,4-dimethylacridone derivatives as modulating agents, vinblastine has shown IC_{50} value of about 3.2 ± 0.12 nM against MCF7 and 69.3 ± 0.02 nM against MCF7/ADR cell lines respectively. This study identified that nature of surrounding tertiary amine and length of alkyl side chain for 2,4-dimethylacridones have shown profound impact on cytotoxicity, ability to modulate in drug resistant cell line.

The presence of β-hydroxyethyl piperazine as secondary amine was found interesting, has shown IC_{50} of 12 ± 0.04 µM with propyl side chain (**11f**), 2 ± 0.03 µM with butyl side chain (**12f**) against human MCF7 cell line and IC_{50} of 15.1 ± 0.11 µM with propyl side chain and 2.56 ± 0.05 µM with butyl side chain against MCF7/ADR cell line, IC_{50} of 8 ± 0.03 nM with propyl side chain and 1.25 ± 0.05 nM with butyl side chain against MCF7/ADR cell line with vinblastine at IC_{10} concentration of modulators. Among the series of 2,4-dimethylacridones, compounds with butyl side chain have shown better cytotoxicity profile compared to propyl side chain. Comparison of length of alkyl side chain *vs* cytotoxicity, more interesting thing observed was acridones with butyl side chain have shown complete reversal of resistance against MCF7/ADR cell line with vinblastine at IC_{10} concentration of modulator, irrespective of secondary amine attached. Results suggests that length of alkyl side chain plays a critical role and essential for the acridones in reversal of MDR mediated through transporter ABCB1. Evidence to that is increased cytotoxicity against MCF7/ADR cell line of acridones with butyl side chain i.e., long lipophilic group might be helping in interaction of membrane bound transporter P-gp.

2.2.2 Photolabeling studies with [^{3}H]-Azidopine

Photoaffinity labelling of P-glycoprotein is the best and frequently used method to identify whether the compound has ability to be a P-gp substrate. In general, compounds which can compete for the active binding site of transporters responsible for multidrug resistance with azidopine will block the photolabelling. For example, drugs like vincristine, vinblastine or verapamil has the ability to completely block the binding of photolabelled azidopine with the active site of P-gp [28]. In the present study, to identify the possible mechanism and strength of inhibition, competition between [^{3}H]-azidopine and the 2,4-dimethylacridones was observed.

Literature suggests that KB-VI cells are also one of the multidrug resistant variant which can exhibits high level resistance to colchicine, Adriamycin or vinblastine mediated through P-glycoprotein compared to MCF7/ADR cells. Experimental study identified that multidrug resistant KB cell lines have amplified two related DNA sequences which are homologous to the Chinese hamster mdr gene. Also resistant KB cell lines have exhibited high specificity to vinblastine which can be photoactivated to quantify the affinity of acridones to P-gp [29-31].

Bruggemann et al., experimental study identified that P-gp from human KB cells with high concentration of colchicine contains valine residue at position 185 and with high concentration of vinblastine or Adriamycin retains glycine residue at position 185. These two cell lines show different pattern of binding for vinblastine and clearly suggests that amino acid residue at 185 position is essential for binding or transport of drugs by P-gp. Hence, we have performed azidopine photolabelling of title compounds with well known, selective and potent modulator of P-gp verapamil [32].

Table 3. Interaction of acridones with P-gp by photolabeling with [^{3}H]-Azidopine

Compound Code	Percentage of control (%)
10	33
11	28
11a	26
11b	34
11c	46
11d	36
11e	40
11f	52
12	36
12a	36
12b	42
12c	43

12d	54
12e	55
12f	58
Verapamil (Std.)	61

Our experiment identified that all the synthesized compounds have shown appreciable results by competing with azidopine at the active site of protein i.e., P-gp and is identified with reduced photoaffinity (**Table 3**). Observation of the experimental results suggests that acridone with butyl side chain have displayed better competition than that of acridones with propyl side chain might be because of hydrophobicity. Photolabelling studies identified that verapamil has shown better competition than all of the title compounds. An attempt has been made to identify the structure activity relationship of 2,4-dimethylacridones with propyl and butyl side chain and MDR modulation ability. Butyl series of acridones have shown appreciable results compared to propyl series. To further identify the effect of alkyl side chain length, we are planning for pentyl and hexyl alkyl side chain of title compounds. Results suggests that MDR modulation of 2,4-dimethylacridones might be mediated through P-gp transporter mechanism.

2.3 Computational Studies:

2.3.1 *In silico* prediciton of physicochemical properties

Physicochemical properties of title compounds have been predicted virtually based on theoretical approaches to identify the compounds which violate the optimum parameters required for the drug likeness and anti-proliferative activity. Log P values obtained were quite different, acridones with propyl side chain ranging from 2.37 to 4.42 and acridones with butyl side chain ranging from 2.84 to 4.68. All the title compounds have passed for Lipinski's rule of five, which increases the scope for the extension of active compounds to *in vivo* screening. Descriptors like Polar Surface Area (PSA), QPlogP o/w (Predicted octanol/water partition coefficient), pKa, QPPCaco (Predicted apparent Caco-2 permeability in nm/sec), QPlogBB (Predicted brain/blood partition coefficient), QPPMDCK (Predicted apparent MDCK cell permeability in nm/sec) were calculated and results were given in **Table 4**.

Lipophilicity is one of the fundamental molecular property and important parameter in the design of drugs. Especially lipophilicity plays a major role in the anticancer activity, but there are potent and active molecules which exhibit anticancer activity with low lipophilicity and high molecular weight [33-37]. In the present study, we have calculated the logP by Schrodinger software to identify the relationship of lipophilicity of acridones and anticancer activity. Here, the series of acridone derivatives contains propyl and butyl alkyl side chain with tertiary amines as essential pharmocophoric structures for cytotoxicity like morpholinyl, piperidinyl, *N*-methylpiperazinyl, *N*-diethylamino, *N*-diethanolamino, *N*-[(β-hydroxylethyl)]piperazino, etc. Compound 10-(4-*N*-piperidinobutyl)-2,4-dimethylacridone (**12b**) was identified most lipophilic and 10-(3-[*N*-diethanolamino] propyl)-2,4-dimethylacridone (**11e**) less lipophilic. Both the compounds were not active and thus, the lipophilicity of the title compounds seems to contribute anticancer activity to some extent.

Table 4. Molecular descriptors of acridone derivatives

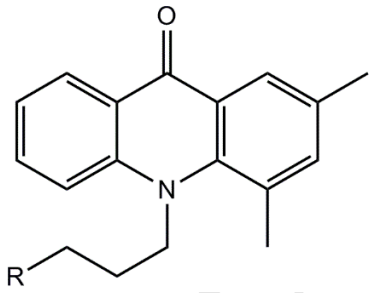

11a-f

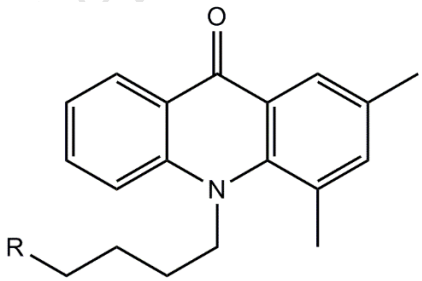

12a-f

Compound Code	R	Mol. Wt.	PSA	pKa	QPlog Po/w	QPP Caco	QPlogBB	QPP MDCK
11a	Morpholinyl	350.46	45.084	7.26	3.278	900.68	0.272	488.79
11b	Piperidinyl	348.48	35.8	9.4	4.426	910.09	0.257	494.31
11c	N-methyl piperazinyl	363.50	41.806	8.2	3.115	195.82	0.586	103.92
11d	N-diethyl amino	336.47	33.741	9.8	4.18	913.66	0.161	496.41
11e	N-diethanol amino	368.47	75.6	9.0	2.37	168.91	-0.838	80.06
11f	N-[(β-	393.52	61.293	7.9	2.583	78.09	-0.041	38.47

	hydroxyethyl)] piperazino							
12a	Morpholinyl	364.48	45.12	7.8	3.677	897.108	0.195	486.69
12b	Piperidinyl	362.51	35.101	10.3	4.684	876.67	0.178	474.72
12c	N-methyl piperazinyl	377.52	41.837	10.7	3.521	194.901	0.499	103.39
12d	N-diethyl amino	350.50	34.061	10.7	4.623	927.261	0.085	504.405
12e	N-diethanol amino	382.50	76.298	9.3	2.847	171.02	-0.979	81.14
12f	N-[(β-hydroxyethyl) piperazino	407.55	63.592	8.4	2.915	59.904	-0.266	28.88

pKa is also one of the important and fundamental property to be considered for the design of effective anticancer compounds. Charge of the molecule i.e., pKa is related to many properties like solubility, permeability, distribution, protein binding, metabolism, excretion, etc. Physiology of tumor and pKa of the molecule are essential which in turn effects the cellular uptake and retention of compounds [38]. In silico method was employed to predict the pKa of acridones by ACD labs/pKa DB software and observed in the range of 7.26-10.7 [39-43]. Substitution of acridones with secondary amines have great impact on pKa and makes the molecule exist in both ionized and unionized forms. Experimental determination of pKa for selected anticancer drugs have identified that majority of drugs have pKa in the range of 8 to 10. In comparison of pKa with *in vitro* cytotoxicity of acridone derivatives, active compounds **12f, 12e, 12d, 11f** have pKa values 8.4, 9.3, 10.7, 7.9. Poor correlation was observed between anticancer activity and pKa. Experimental observation might give a better correlation and present study suggests that pKa is one of the essential parameter to be considered for design of effective anticancer agent, might not be sole property.

Molecular weight and polar surface area of compounds were in the range of 336.47 to 407.55 and 33.74 to 76.29, optimum with respect to number of hydrogen bonding donors and acceptors. Other descriptors like QPPCaco which predicts the apparent permeability across the Caco-2 cell

membrane which represents the gut-blood barrier through non-active transport were calculated. Recommended values of QPPCaco as per software are <25 poor permeability and >500 is more permeability. None of the title compounds have poor Caco permeability and 6 out of 12 compounds have more than 900. QPlogBB represents the brain/blood partition coefficient and QPPMDCK represents the apparent permeability across the MDCK cells which can be considered as good mimic for Blood Brain Barrier (BBB) by non-active transport. In summary, Qikprop predictions suggests that 2,4-dimethylacridone with propyl or butyl chain and substitution of various secondary amines have optimum parameters for anticancer activity and can be considered as lead molecule for further modifications.

2.3.2 Molecular docking

To identify the potential structural features for cytotoxicity and interaction at active site of P-gp, molecular docking studies have been performed. Compounds have shown better hydrogen binding interactions and are comparable to control molecules. Along with *in vitro* results, docking studies too confirmed that alkyl side chain is essential for anticancer activity and length of alkyl side chain, chemistry of secondary amine plays crucial role for efficient binding at the active site. Studies revealed that H-bonding and hydrophobic interactions are the key factors for binding with P-gp. Molecular docking results indicating docking score, energy, interacting residues at the binding site of P-gp were summarized in **Table 5**. Along with that binding interactions i.e., docked poses of least and most active compounds were represented in **Figure 3** and **Figure 4**.

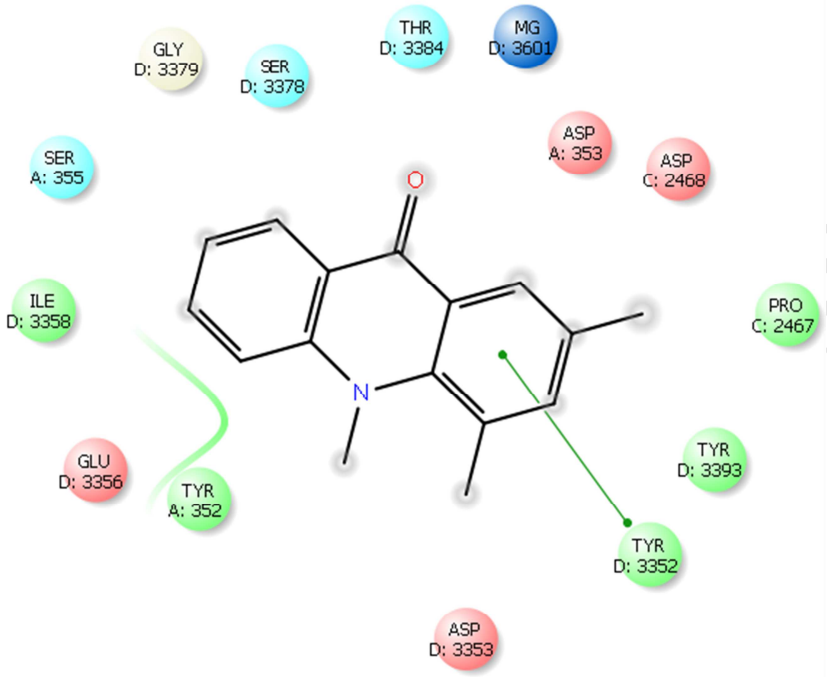

Figure 3. 2D interaction diagram of compound **10** with P-gp

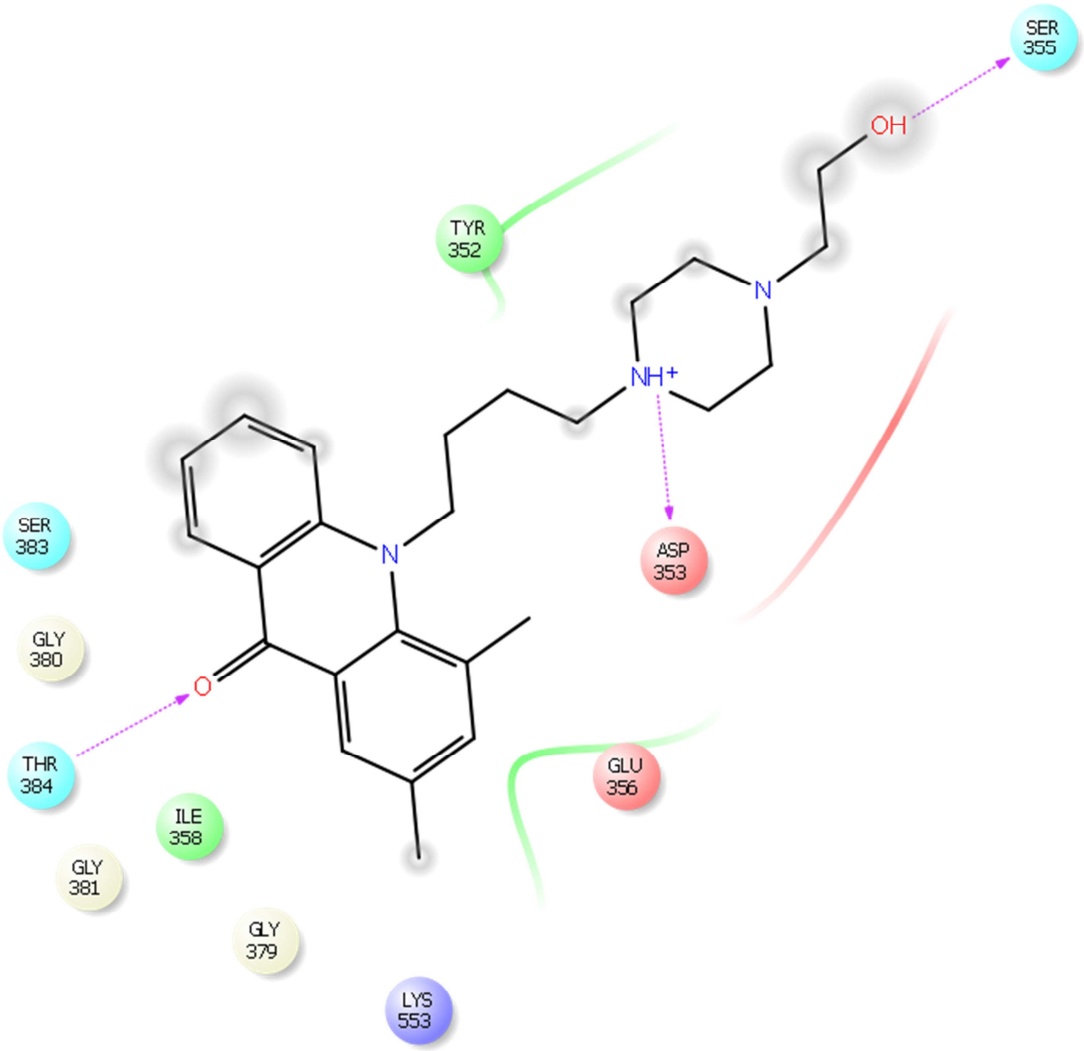

Figure 4a. 2D interaction diagram of compound **12f** with P-gp

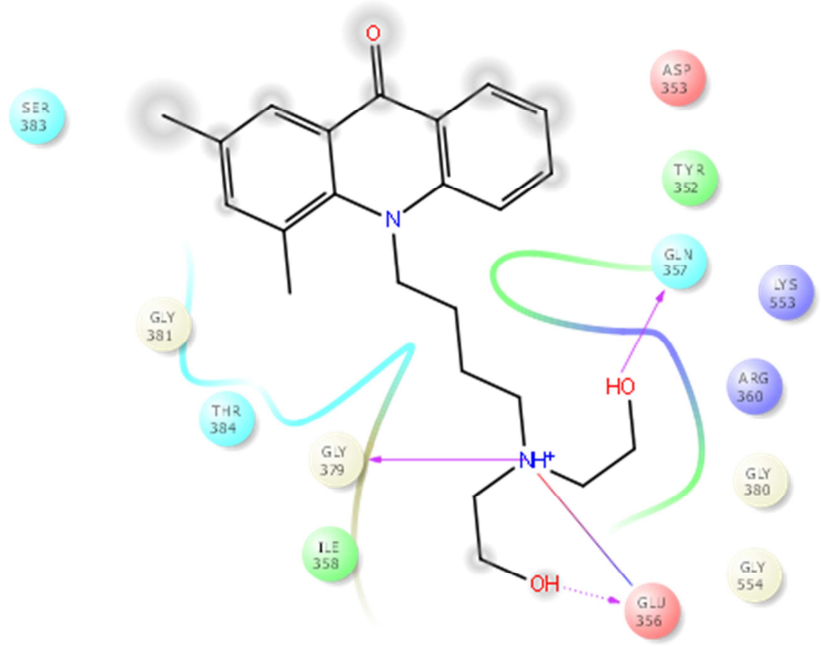

Figure 4b. 2D interaction diagram of compound **12e** with P-gp

Figure 4. 2D interaction diagram of compounds with P-gp

Binding interactions of all the 12 compounds were analyzed and identified that unsubstituted acridone **10** was found with least score indicating that side chain is essential (**Figure 3**). Binding interactions of compound **12e** at the active binding site of P-gp shows that both the hydroxyl groups of secondary amine *N*-diethanolamine has formed hydrogen bonds with Glu356 and Gln357, nitrogen of amine found interacting with Glu356 and Gly379. Presence of two hydroxyl groups in the secondary amine might have improved the binding affinity at the active site of P-gp and displayed good docking score -6.426 kcal/mole among the series. Similarly compound **11e**, acridone with propyl side chain containing *N*-diethanolamine has exhibited better binding affinity with docking score -6.389 kcal/mole. Two hydroxyl groups of compound formed

hydrogen bonding with Glu356 and Gln357, nitrogen of *N*-diethanolamine with Gly379, π-π stacking of acridone ring with Tyr352.

The binding interactions of the active compound **12f** i.e., acridone with butyl side chain containing β-hydroxy piperazine from *in vitro* cytotoxicity shows that hydroxyl group of secondary amine forms hydrogen bonding with Ser355, nitrogen of secondary amine with Asp353 and oxygen of acridone ring with Thr384 (**Figure 4a**). Molecular docking score of compound **12f** is -5.324 kcal/mol. The binding interaction of active compound **12d** i.e., acridone with butyl side chain containing *N*-diethylamino shows that nitrogen of secondary amine forms hydrogen bonding with Glu356 and Gly379. Compounds **11e** and **12e** with top ranking docking score have shown similar binding interactions with Gln357, Glu356 and Gly379. Moreover active compounds of *in vitro* results have not shown similar binding interactions with that of compounds **11e** and **12e**.

The binding interactions of compound **12c** i.e., acridone with butyl side chain containing *N*-methyl piperazine have displayed least molecular docking score -3.964 kcal/mol shows that nitrogen of secondary amine forms hydrogen bonding with Glu356 and Gly379, π-π stacking of acridone ring with Tyr352. Present study identified that chemical nature of secondary amine substituted at the end of alkyl chain plays an essential role in cytotoxicity and MDR modulation. **12e** and **11e** have shown better docking scores compared to **12f** and **11f**. **12e** and **11e** have the common secondary amine *N*-diethanolamine whereas **12f** and **11f** with *N*-[(β-hydroxyethyl)]piperazine. Compounds **12e (Figure 4b)** with highest docking score of -6.426 might be because of presence of two hydroxyl groups of secondary amine improved the binding interactions at the target site and **12f** the most active compound with docking score -5.324 at the active site of P-gp. Similarly compound **11e** have shown docking score -6.389 might be because of secondary amine. Poor correlation was observed between the predicted log P of title compounds and in vitro cytotoxicity. To further investigate the mechanism, experimental determination of lipophilicity might help in better understanding. Interestingly title compounds have shown better interactions than potent and well known P-gp modulator verapamil. Experimental and molecular studies clearly suggests that acridones with alkyl side chain and hydroxyl substituted secondary amine are essential for multidrug resistance (MDR) reversing agents.

Table 5. Molecular docking results of acridones with the target protein P-gp

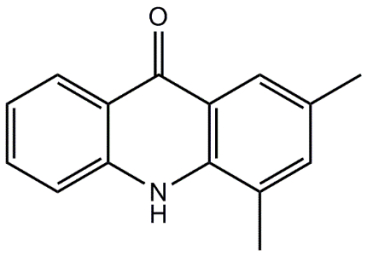

10

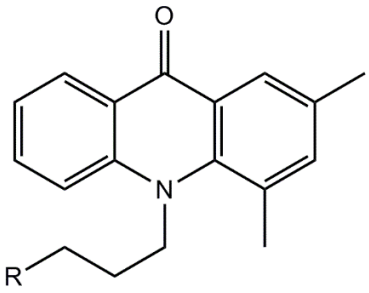

11a-f

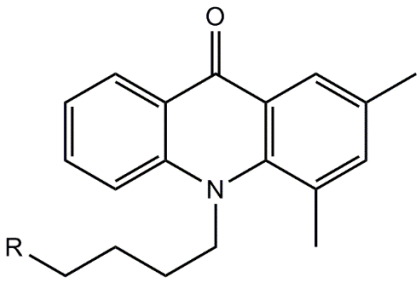

12a-f

Compound Code	R	Glide SP Score	Glide SP emodel	Amino acid residues in interaction
11a	Morpholinyl	-4.688	-60.097	Thr384, Asp353
11b	Piperidinyl	-4.364	-51.356	Thr384, Glu356
11c	N-methyl piperazinyl	-4.484	-56.669	Tyr352, Glu356, Gly379
11d	N-diethyl amino	-4.493	-50.986	Gly379, Glu356
11e	N-diethanol amino	-6.389	-69.655	Tyr352, Gly379, Glu356, Gln357
11f	N-[(β-hydroxyethyl)] piperazino	-4.809	-70.699	Thr384, Glu356
12a	Morpholinyl	-4.791	-60.478	Tyr352, Asp353, Glu356
12b	Piperidinyl	-4.722	-58.556	Tyr352, Glu356
12c	N-methyl piperazinyl	-3.964	-52.468	Tyr352, Glu356, Gly379
12d	N-diethyl amino	-4.394	-56.913	Tyr352, Glu356, Asp353
12e	N-diethanol amino	-6.426	-73.943	Gln357, Glu356, Gly379
12f	N-[(β-hydroxyethyl) piperazino	-5.324	-77.199	Thr384, Asp353, Ser355
Std.	Verapamil	-4.054	-67.145	Asp353, Tyr352

2.3.3 **QSAR descriptors**

Correlation of the molecular descriptors and biological activity is essential to identify and understand the Structure Activity Relationship (SAR) [44-50]. Can be achieved by considering the most significant and minimum molecular descriptors for the anticancer activity to get a best fit. A good number of online tools are available to calculate the molecular descriptors i.e., chemical descriptors like surface area, volume, charge, dipole moment and molecular property descriptors like lipophilicity.

2.3.3.1 Exploring and Selection of descriptors

All the 12 acridone derivatives were prepared by standard protocol using Ligprep module and submitted to Qikprop module for the prediction of molecular descriptors. Data pertaining to compounds with ID and name of structure were composed in the software. Under the section of dependent variable i.e., activity, results obtained from the *in vitro* cytotoxicity screening against MCF7 were expressed in the form of $\log(1/IC_{50})$ for convenience. The next critical step is selection of essential descriptors to simplify the data and to build a strong model which can identify the safe and potent molecule. From the data generated by the Qikprop module of Schrodinger, 15 descriptors [log P, pKa, molecular weight, hydrogen bonding acceptors (HbA), hydrogen bonding donors (HbD), square of dipole moment divided by the molecular volume (dip^2/V), Van der Waals surface area of polar nitrogen and oxygen atoms and carbonyl carbon atoms (PSA), total solvent accessible surface area in angstroms using a probe with 1.4 A^0 radius (SASA), hydrophobic component of the SASA- saturated carbon and attached hydrogen (FOSA), hydrophilic component of the SASA- SASA on N, O, H on heteroatoms and carbonyl C (FISA), π component of SASA- carbon and attached hydrogen (PISA), total solvent-accessible volume in cubic angstroms using a probe with 1.4 A^0 radius (volume), globularity descriptor- $(4\pi r^2)/(SASA)$ (glob), PM3 calculated Ionization potential- negative of HOMO energy (IP) and PM3 calculated Electron affinity- negative of LUMO energy (EA)] were shortlisted for building a QSAR model. The abbreviations and description of molecular descriptors were taken from the Qikprop user manual of Schrodinger software.

BuildQSAR software offers two ways for selection of suitable descriptors to generate a QSAR equation. One way is to randomly select the descriptors, build a model and validate by identifying the values correlation coefficient R and R^2. BuildQSAR program has an option to search, compare and build a best model with one to five variables using two approaches i.e., systematic search and genetic algorithm based search. This method identifies the potential molecular descriptors and also better model can be selected from the value of correlation coefficient R. Additionally, this method has an option to do cross-validation by Leave-One-Out (LOO) method and also not to show "Not Predictable" models. The other way is to plot a graph and identify the degree of correlation between dependent variables i.e., biological activity and independent variables called molecular descriptors [51].

Better model can be designed by identifying the essential molecular descriptors. Building a model with the selection of few molecular descriptors cannot identify or predict the active molecule, similarly with large number of descriptors will shows errors and generates a model with less accuracy [52]. Taking that into consideration, BuildQSAR software has an option to correlate maximum five variables by both systematic and genetic algorithm based search and helps to identify the significant molecular descriptors for building a better model. The quality and accuracy of the model can be identified from the following characteristics correlation coefficient (R), high squared correlation coefficient (R^2), high Fischer's value (F-test), standard error of estimate (s), statistical significance > 99.9% with Fischer's statistic- F value (p), cross validated squared correlation coefficient (Q^2), standard deviation of sum of squared error of prediction (S_{PRESS}), standard deviation of error of prediction (SDEP). The predictive ability of model can be identified from the value of correlation coefficient R and R^2 i.e., higher the value most accurate, highest F value or lowest standard deviation. From the results obtained by systematic search of four and five variables, R value was in the range of 0.901 to 0.937. Analyzing the results shows that pKa, FOSA, FISA, PISA, volume and dip^2/V were essential descriptors. Similarly by genetic algorithm based search has shown R values in the range of 0.946 to 0.977. The genetic algorithm based search has shown better correlation coefficient values with 0.977 and 0.966 with five variables and 0.946 with four variables. And the significant variables from genetic algorithm were log P, pKa, HbA, IP, PISA, dip^2/V.

2.3.3.2 Building QSAR model

Previous step identified the potential and significant molecular descriptors by two approaches i.e., systematic search and genetic algorithm based search. Based on the six molecular descriptors identified from systematic search and genetic algorithm based approaches, model 1 and model 2 were generated. Furthermore by combining the descriptors from model 1 and model 2, model 3 was built with nine variables (**Table 6**). The biological activity and identified descriptors from the respective models were submitted to BuildQSAR program to generate QSAR equation by the approach of Multiple Linear Regression (MLR) analysis (**Table 7, Table 8, Table 9**). The equations obtained from the respective models were shown in **Table 11**. For the generated models, software gives predicted activity, residual activity i.e., difference between observed and predicted activity and standard deviation of residual activity. Also provides the correlation analysis of observed activity *vs* predicted activity for all the three generated models (**Figure 5, Figure 6, Figure 7**). Best correlation was observed for all the three models generated by software with minimum deviations (**Table 10**).

Table 6. Molecular descriptors of QSAR models

S. No.	No. of descriptors	Molecular descriptors
Model 1	06	pKa, FOSA, FISA, PISA, volume, dip^2/V
Model 2	06	log P, pKa, HbA, IP, PISA, dip^2/V
Model 3	09	log P, pKa, HbA, IP, volume, FOSA, FISA, PISA, dip^2/V

Table 7. Molecular descriptors data submitted to build Model 1

Compound code	log(1/IC_{50})	pKa	FOSA	FISA	PISA	Volume	dip^2/V
11a	1.772	7.260	385.008	46.212	214.717	1164.610	0.022
11b	1.763	9.400	416.726	45.736	214.717	1210.045	0.023
11c	1.700	8.200	428.259	52.496	211.815	1249.937	0.020
11d	1.464	9.800	392.819	45.557	209.614	1176.229	0.031
11e	1.282	9.000	332.330	122.866	209.450	1212.221	0.044
11f	1.079	7.900	415.279	94.596	211.282	1308.793	0.041
12a	1.301	7.800	417.417	46.394	215.932	1225.708	0.015

12b	1.478	10.300	434.668	47.449	212.851	1254.774	0.028
12c	1.161	10.700	463.986	52.714	215.027	1311.894	0.020
12d	0.919	10.700	430.885	44.880	213.842	1242.559	0.027
12e	0.602	9.300	381.130	122.296	215.019	1292.345	0.016
12f	0.301	8.400	438.003	106.743	213.849	1375.778	0.021

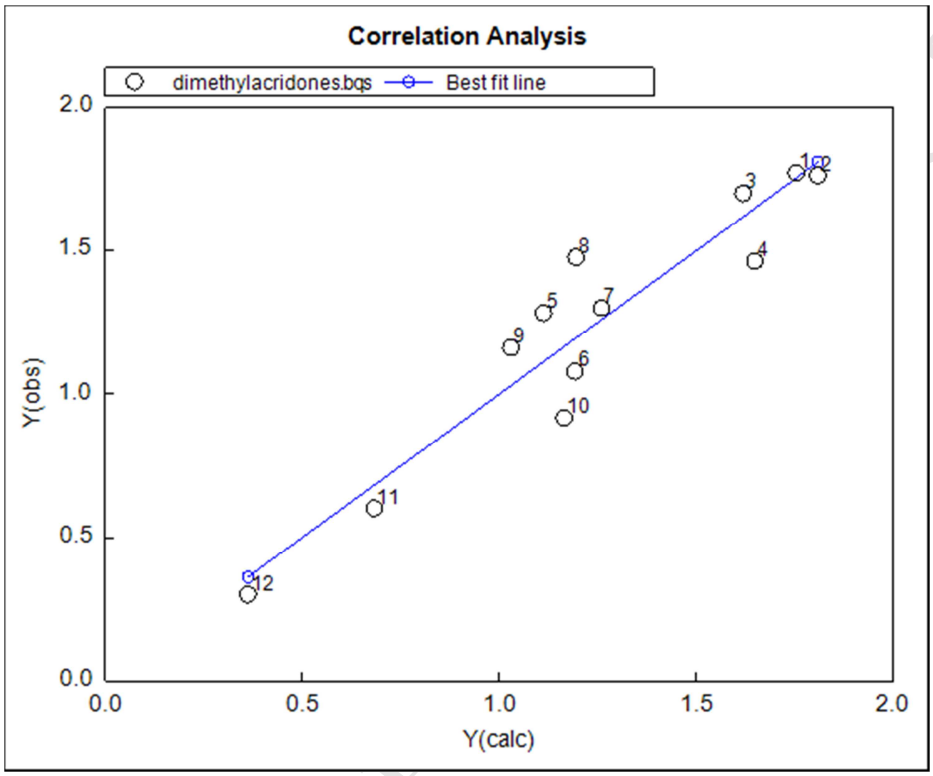

Figure 5: Correlation analysis of predicted and observed biological activity of Model 1

Table 8. Molecular descriptors data submitted to build Model 2

Compound code	log(1/IC_{50})	log P	pKa	PISA	HbA	dip^2/V	IP
11a	1.772	3.278	7.260	214.717	6.200	0.022	8.320
11b	1.763	4.426	9.400	214.717	4.500	0.023	8.271
11c	1.700	3.115	8.200	211.815	6.500	0.020	8.297
11d	1.464	4.180	9.800	209.614	4.500	0.031	8.138

11e	1.282	2.370	9.000	209.450	7.900	0.044	8.155
11f	1.079	2.583	7.900	211.282	8.200	0.041	8.131
12a	1.301	3.677	7.800	215.932	6.200	0.015	8.324
12b	1.478	4.684	10.300	212.851	4.500	0.028	8.154
12c	1.161	3.521	10.700	215.027	6.500	0.020	8.301
12d	0.919	4.623	10.700	213.842	4.500	0.027	8.155
12e	0.602	2.847	9.300	215.019	7.900	0.016	8.304
12f	0.301	2.915	8.400	213.849	8.200	0.021	8.172

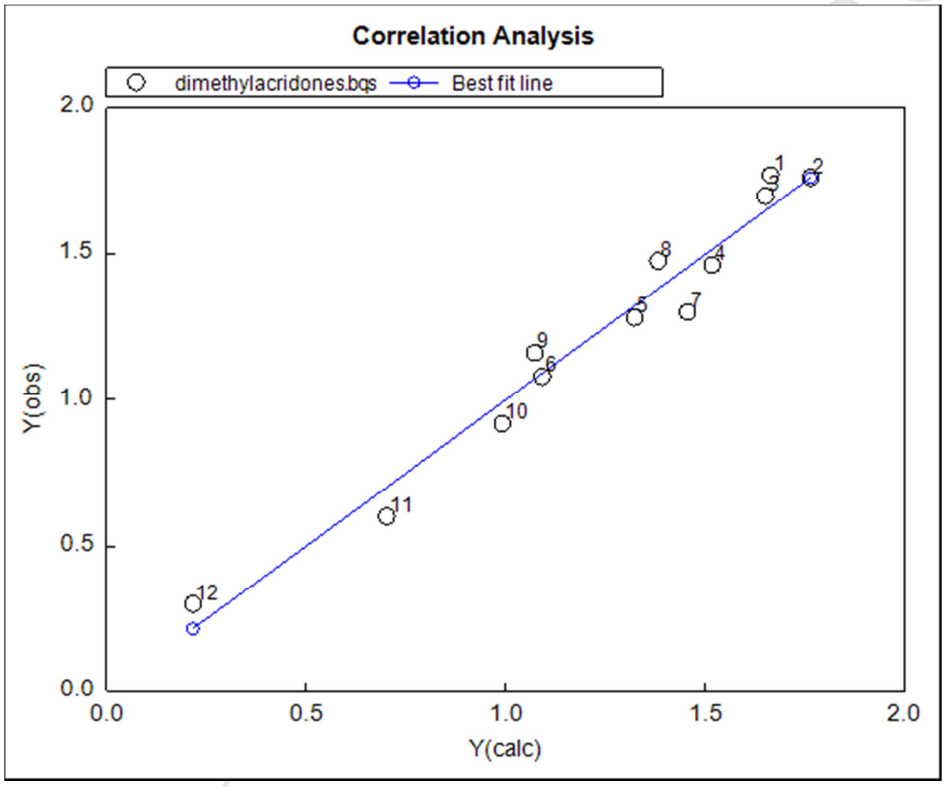

Figure 6: Correlation analysis of predicted and observed biological activity of Model 2

Table 9. Molecular descriptors data submitted to build Model 3

Comp. code	log(1/IC_{50})	log P	pKa	FOSA	FISA	PISA	Volume	HbA	dip^2/V	IP
11a	1.772	3.278	7.260	385.008	46.212	214.717	1164.610	6.200	0.022	8.320
11b	1.763	4.426	9.400	416.726	45.736	214.717	1210.045	4.500	0.023	8.271

11c	1.700	3.115	8.200	428.259	52.496	211.815	1249.937	6.500	0.020	8.297
11d	1.464	4.180	9.800	392.819	45.557	209.614	1176.229	4.500	0.031	8.138
11e	1.282	2.370	9.000	332.330	122.86	209.450	1212.221	7.900	0.044	8.155
11f	1.079	2.583	7.900	415.279	94.596	211.282	1308.793	8.200	0.041	8.131
12a	1.301	3.677	7.800	417.417	46.394	215.932	1225.708	6.200	0.015	8.324
12b	1.478	4.684	10.300	434.668	47.449	212.851	1254.774	4.500	0.028	8.154
12c	1.161	3.521	10.700	463.986	52.714	215.027	1311.894	6.500	0.020	8.301
12d	0.919	4.623	10.700	430.885	44.880	213.842	1242.559	4.500	0.027	8.155
12e	0.602	2.847	9.300	381.130	122.29	215.019	1292.345	7.900	0.016	8.304
12f	0.301	2.915	8.400	438.003	106.74	213.849	1375.778	8.200	0.021	8.172

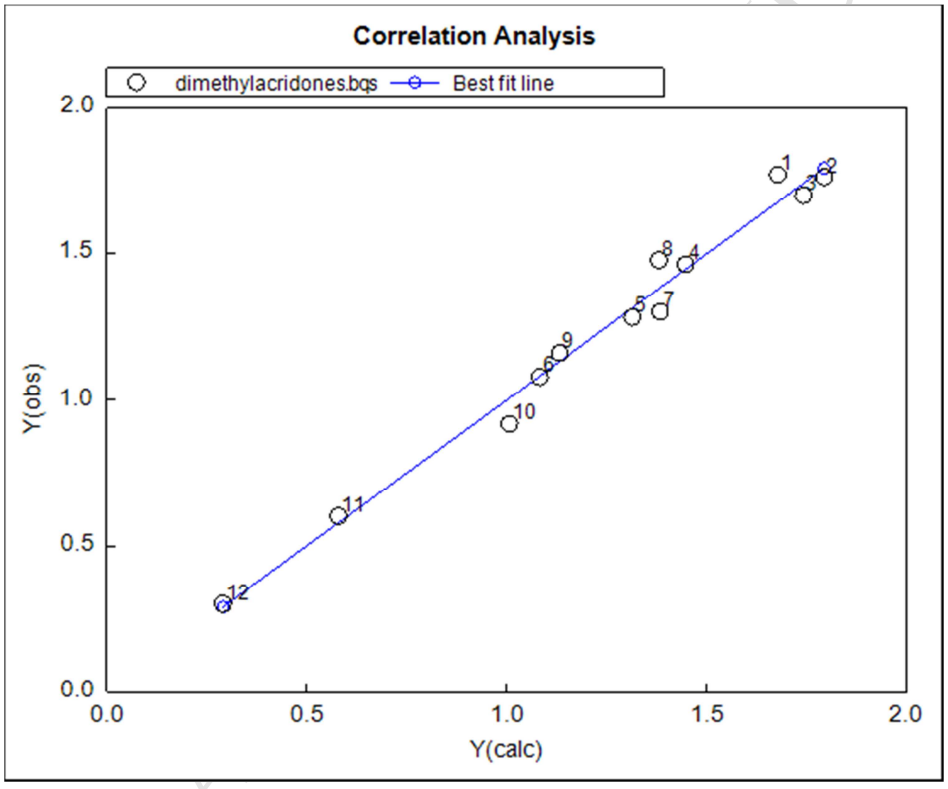

Figure 7: Correlation analysis of predicted and observed biological activity of Model 3

Table 10. Residual Table of QSAR models

Comp. code	Model 1			Model 2			Model 3		
	Activity (obs)	**Activity (calc)**	**Activity (res)**	**Activity (obs)**	**Activity (calc)**	**Activity (res)**	**Activity (obs)**	**Activity (calc)**	**Activity (res)**
11a	1.772	1.753	0.019	1.772	1.663	0.109	1.772	1.677	0.095
11b	1.763	1.808	-0.045	1.763	1.763	0.000	1.763	1.793	-0.030
11c	1.700	1.618	0.082	1.700	1.650	0.050	1.700	1.741	-0.041
11d	1.464	1.648	-0.184	1.464	1.517	-0.053	1.464	1.446	0.018
11e	1.282	1.112	0.170	1.282	1.322	-0.040	1.282	1.313	-0.031
11f	1.079	1.192	-0.113	1.079	1.091	-0.012	1.079	1.082	-0.003
12a	1.301	1.259	0.042	1.301	1.455	-0.154	1.301	1.383	-0.082
12b	1.478	1.194	0.284	1.478	1.381	0.097	1.478	1.380	0.098
12c	1.161	1.029	0.132	1.161	1.072	0.089	1.161	1.132	0.029
12d	0.919	1.164	-0.245	0.919	0.991	-0.072	0.919	1.006	-0.087
12e	0.602	0.682	-0.080	0.602	0.701	-0.099	0.602	0.579	0.023
12f	0.301	0.362	-0.061	0.301	0.216	0.085	0.301	0.290	0.011

Table 11. QSAR equations for respective models

S. No.	QSAR equation
Model 1	$\log(1/IC_{50})$ = - 0.1697 (± 0.1878) pKa + 0.0878 (± 0.0936) FOSA + 0.0823 (± 0.0958) FISA - 0.0399 (± 0.1451) PISA - 0.0514 (± 0.0512) Volume + 9.8022 (± 34.8679) dip 2/V + 33.5783 (± 38.8613)
Model 2	$\log(1/IC_{50})$ = + 1.3337 (± 1.6461) log P - 0.1718 (± 0.1261) pKa - 0.2153 (± 0.1934) PISA + 0.3443 (± 0.7572) HbA + 56.1967 (± 32.0053) dip 2/V + 10.5961 (± 6.1440) IP - 46.7823 (± 31.0711)
Model 3	$\log(1/IC_{50})$ = + 0.1108 (± 4.9092) log P - 0.2059 (± 0.3150) pKa - 0.0479 (±

	0.2578) FOSA - 0.0436 (± 0.2371) FISA - 0.1418 (± 0.4157) PISA + 0.0330 (± 0.1632) Volume - 0.5695 (± 3.5258) HbA + 72.7928 (± 96.3054) dip 2/V + 12.0199 (± 15.9472) IP - 82.7725 (± 187.7604)

2.3.3.3 Analyzing QSAR model

Study was performed by taking respective descriptors and three QSAR models were generated. All the three models have shown very good correlation coefficients 0.943, 0.982 and 0.992. From the **Table 12** it can be identified that Model 3 is showing very high R value 0.992. Among the three models produced, Model 2 can be considered as best one with 0.982 and 0.964 as R and R^2 values. In comparison with other constituents, Model 2 is showing least standard deviation (s) and p value as 0.128 and 0.0018, highest F and Q^2 values as 22.541 and 0.757. Similarly, Model 2 is showing least SPress and SDEP values as 0.334 and 0.225 among the three models. Also Model 2 was generated with six molecular descriptors whereas Model 3 was built with nine descriptors. The present QSAR identified that for acridone derivatives to exhibit cyctotoxicity against MCF7 cell line, molecular descriptors log P, pKa, HbA, IP, PISA, dip^2/V were essential. Results of the study gain possible insights which governs cytotoxic activity and might help in identifying the suitable, potent and safe therapeutic hits.

Table 12. Analysis of QSAR models

S. No	Constituents of QSAR model								
	n	R	R^2	s	F	p	Q^2	SPress	SDEP
Model 1	12	0.943	0.889	0.226	6.700	0.0272	0.377	0.536	0.361
Model 2	12	0.982	0.964	0.128	22.541	0.0018	0.757	0.334	0.225
Model 3	12	0.992	0.983	0.138	13.177	0.0725	0.385	0.841	0.359

3 Experimental:

3.1 Materials & Methods:

All the chemicals utilized for the present study were purchased from the producers such as Sigma-Aldrich, VWR International and Fischer etc., were used without further processing like

purification. Solvents were used directly unless specified. All the reactions were carried out strict anhydrous conditions by passing N_2 gas and progress of reactions was monitored by Thin Layer Chromatography using silica gel 60 F_{254} coated of analytical grade from Merck. All the title compounds were purified by passing through column chromatography packed with silica gel of 230-400 mesh, 60 A^0 of Merck using the solvent system chloroform/methanol (9:1). Melting point of the compounds was determined on Tempirol hot stage and are uncorrected. Pure compounds were characterized by recording UV spectra of Shimadzu-UV-1601 in methanol as solvent, ^{1}H-NMR and ^{13}C-NMR were recorded in Bruker drx 500 MHz Fourier transform NMR spectrometer in DMSO-d_6 as solvent and tetra methyl silane as internal standard. Chemical shifts relative to deuterated solvent were expressed in parts per million (ppm). Chemical information like molecular weight of title compounds was determined by obtaining ESI-MS spectroscopy using methanol as solvent. MS/MS spectra of selected fragments were obtained for the confirmation of drug structure.

3.2 Chemistry: Synthesis of 2,4-dimethyl-N^{10}-substituted acridones

3.2.1 Ullmann's condensation [53]: Preparation of 2-[(2,4-dimethylphenyl)amino]benzoic acid (9)

o-chlorobenzoic acid **7** (5 g, 0.032 mol), 2,4-dimethylaniline **8** (3.97 ml, 0.032 mol) and copper powder (0.2 g) were mixed well in 30 ml of isoamyl alcohol and anhydrous K_2CO_3 (4.41 g) was added to it. Then the contents were mixed and kept for refluxing on oil bath for 6 hrs. The isoamyl alcohol was removed under vacuum and poured into hot distilled water (1 litre), acidified with conc. HCl. The precipitate of crude was filtered and washed with hot distilled water. Later crude acid was neutralized with aq. NaOH, boiled with activated charcoal and filtered. Compound was precipitated out by acidification with conc. HCl, washed with hot distilled water and recrystallized from aqueous methanol gave light yellow solid (yield 27.02 %, mp 175 ^{0}C).

3.2.2 Cyclization of compound 9 to 2,4-dimethylacridone (10)

To compound **9** (6 g) in a 250-mL round bottom flask (RBF), polyphosphoric acid (PPA) (60 g) was added. The contents of the flask were mixed well and kept for heating on water bath at 100 ^{0}C for 3 hrs. Appearance of yellow color in the flask indicated completion of cyclization. The

reaction mixture was transferred into hot distilled water (1 L) and collected. The product (**10**) was recrystallised from HOAc.

Yield: 68%; mp: 318 ^{0}C; ^{1}H-NMR (500 MHz, [D_6]DMSO): 7.1-8.4 (m, Ar-H, 6H), 8.22 (d, 1H, H8, *J* = 8 Hz), 2.37 (s, 3H, CH_3), 2.52 (s, 3H, CH_3), 10.56 (s,1H, NH); ^{13}C-NMR (100 MHz, [D_6]DMSO): 20.66 (C_2- CH_3), 17.75 (C_4- CH_3), 178.54 (C_9), 142.12 ($C_{10'}$, $C_{4'}$), 138.80 ($C_{8'}$, $C_{9'}$), 136.55 (C_7), 131.68 (C_5), 130.67 (C_6), 126.94 (C_3), 121.92 (C_1), 119.75 (C_8), 118.52 (C_4), 116.97 (C_2)'; MS (ESI): m/z: 224 $[M+H]^+$

3.2.3 Synthesis of N^{10}-alkylated acridones *via* Phase Transfer Catalysis (PTC)

3.2.3.1 10-(3-*N*-chloropropyl)-2,4-dimethylacridone (11)

To compound **10** (1 g, 0.0021 mol) in tetrahydrofuran (20 mL), 6N KOH (25 mL) and tetrabutylammonium bromide (0.74 g) was added and the reaction mixture was continued stirring at room temperature for 30 min. To it, 1-bromo-3-chloropropane (0.2 mL, 0.0021 mol) was added dropwise and reaction mixture was stirred for 24 hrs at RT. The solvent was evaporated under vacuum and the aqueous portion was extracted with $CHCl_3$ (3X20 mL). All the portions of organic layers were pooled, washed with distilled water and dried (anhyd. Na_2SO_4) and the solvent was evaporated to give the crude product. The residue was further chromatographed with silica gel gave pure compound **11** as yellow solid.

Yield: 46%; mp: 158 ^{0}C; ^{1}H-NMR (500 MHz, [D_6]DMSO): 7.1-8.3 (m, 6H, Ar-H), 8.3 (d, 1H, H8, *J* = 8 Hz), 2.31 (S, 3H, CH_3), 2.66 (S, 3H, CH_3) 10.42 (s,1H, NH), 2.16 (m, 2H, Hl), 4.08 (t, 2H, Hk), 3.56 (t, 2H, Hm), 2.35-2.89 (s, 2-CH3); ^{13}CNMR (100 MHz, [D_6]DMSO): 18.84 (C_4-CH_3), 21.67 (C_2- CH_3), 25.15 (C_1), 178.52 (C_9), 142.12 ($C_{10'}$, $C_{4'}$), 139.82 ($C_{8'}$, $C_{9'}$), 134.64 (C_7), 133.61 (C_5), 130.68 (C_6), 126.04 (C_3), 124.22 (C_1), 121.75 (C_8), 119.46 (C_4), 117.01 (C_2), 65.32 (C_c, C_d), 59.12 (C_a, C_b), 55.81 (C_k), 52.43 (C_m); MS (ESI): m/z: 299.11 $[M+H]^+$.

3.2.3.2 10-(3-*N*-morpholinopropyl)-2,4-dimethylacridone (11a)

10-(3-N-chloropropyl)-2,4-dimethylacridone (**11**) (1 g, 0.0021 mol) was dissolved in ACN (30 mL) to which KI (1.38 g) was added along with K_2CO_3 (2.29 g) and refluxed for 30 min. Then morpholine (1.04 mL) was added to the reaction mixture and subjected to reflux for additional 20 hrs. The contents in the flask were cooled, diluted with distilled water and extracted with $CHCl_3$

(3X20 mL). All the portions of organic layers were combined, washed with distilled water and dried (anhyd. Na_2SO_4) and the solvent evaporated to give the product as oil. The oily residue was further purified by packing column chromatography with silica gel and free base obtained was dissolved in acetone and treated with ethereal HCl to generate stable HCl salt of **11a.**

Yield: 58%; mp: 159 ^{0}C; ^{1}H-NMR (500 MHz, [D_6]DMSO): 7.10-8.71 (m, Ar-H, 6H), 8.22 (d, 1H, H8, *J* = 8 Hz), 2.41 (s, 6H, 2CH_3), 2.61-2.73 (m, 8H, Hc, Hd, He, Hl), 3.44-4.20 (m, 8H, Ha, Hb, Hk, Hm); ^{13}C-NMR (100 MHz, [D_6]DMSO): 178.45 (C9), 143.90 (C9', C8'), 142.01 (C10', C4'), 135.92 (C7), 127.28 (C3), 131.61 (C5), 129.05 (C6), 124.48 (C1), 122.25 (C8), 118.95 (C2), 115.65 (C4), 53.02 (Ck), 52.28 (Cm), 57.14 (Ca, Cb), 64.38 (Cc, Cd), 27.30 (Cl), 22.94 (C2–CH_3), 23.81 (C4–CH3); MS (ESI): m/z: 351.67 $[M+H]^+$, 224, 146.

3.2.3.3 10-(3-*N*-piperidinopropyl)-2,4-dimethylacridone (11b)

The procedure employed for **11a** was replicated with 1 g of **11,** 1.56 g of KI, 2.6 g of K_2CO_3 and 1.2 ml (0.35 mol) of piperidine. The oily residue was further purified by packing column chromatography with silica gel and free base obtained was dissolved in acetone and treated with ethereal HCl to generate stable HCl salt of **11b.**

Yield: 33%; mp: 168 ^{0}C; ^{1}H-NMR (500 MHz, [D_6]DMSO): 7.03-8.16 (m, Ar-H, 6H), 8.21 (d, 1H, H8, *J* = 8 Hz), 2.12-2.41 (s, 2-CH_3, 6H), 2.84-2.91 (m, H_l, H_m 4H), 3.32-4.10 (m, H_k, H_n, H_a, H_b, H_c, H_d, 12H); ^{13}C-NMR (100 MHz, [D_6]DMSO): 17.94 (C_4, CH_3), 21.85 (C_2- CH_3), 26.03 (C_1), 177.95 (C_9), 141.91 ($C_{10'}$, $C_{4'}$), 139.56 ($C_{8'}$, $C_{9'}$), 138.81 (C_7), 137.22 (C_5), 131.15 (C_6), 123.06 (C_3), 121.31 (C_1), 119.34 (C_8), 118.91 (C_4), 116.80 (C_2), 64.52 (C_c, C_d), 58.45 (C_a, C_b), 52.32 (C_k), 23.97 (C_m); MS (ESI): m/z: 349.11 $[M+H]^+$, 291, 224, 211.

3.2.3.4 10-(3-*N*-methylpiperazino)propyl-2,4-dimethylacridone (11c)

The procedure employed for **11a** was replicated with 1 g of **11,** 1.13 g of KI, 2.18 g of K_2CO_3 and 1.22 mL (0.34 mol) of *N*-methylpiperazine. The oily residue was further purified by packing column chromatography with silica gel and free base obtained was dissolved in acetone and treated with ethereal HCl to generate stable HCl salt of **11c.**

Yield: 59%; mp: 152 ^{0}C; ^{1}H-NMR (500 MHz, [D_6]DMSO): 7.12-8.26 (m, Ar-H, 6H), 8.22 (d, 1H, H8, *J* = 8 Hz), 1.76-1.79 (s, 6H, 2CH_3), 2.05-2.47 (m, 10H, Hc, Hd, He, Hl and Hm), 2.47-

2.81 (m, 8H, Ha and Hb, Hk and Hn); ^{13}C-NMR (100 MHz, [D_6]DMSO): 178.65 (C9), 143.72 (C9', C8'), 141.14 (C10', C4'), 135.07 (C1), 134.14 (C7), 127.39 (C3), 126.61 (C5), 124.21 (C6), 122.36 (C8), 118.82 (C2), 117.85 (C4), 55.97 (Ck), 53.54 (Cm), 48.41 (Ca), 46.04 (Cb), 44.32 (Cc, Cd), 28.53 (Ce), 26.28 (Cl), 24.76 (C2–CH3), 22.48 (C4–CH3); MS (ESI): m/z: 365.31 $[M+H]^+$, 351, 224, 215.

3.2.3.5 10-(3-[*N*-diethylamino]propyl)-2,4-dimethylacridone (11d)

The procedure employed for **11a** was replicated with 1 g of **11,** 1.45 g of potassium iodide, 2.42 g of potassium carbonate and 1.17 mL (0.35 mol) of *N,N*-diethylamine. The oily residue was further purified by packing column chromatography with silica gel and free base obtained was dissolved in acetone and treated with ethereal HCl to generate stable HCl salt of **11d.**

Yield: 30%; mp: 137 ^{0}C; ^{1}H-NMR (500 MHz, [D_6]DMSO): 7.12-8.27 (m, Ar-H, 6H), 8.22 (d, 1H, H8, *J* = 8 Hz), 1.74-1.76 (s, 2-CH_3, 6H), 3.12–4.31 (m, 8H, Ha and Hb, Hk and Hm), 2.18 (m, 2H, Hl), 2.81 (s, 6H, 2-CH_3), 1.11–1.40 (m, 6H, Hc, Hd); ^{13}C-NMR (100 MHz, [D_6]DMSO): 178.15 (C9), 143.61 (C9', C8'), 143.77 (C10', C4'), 134.52 (C1), 131.71 (C7), 124.29 (C3), 127.91 (C5), 126.93 (C6), 121.99 (C8), 119.52 (C2), 117.35 (C4), 56.09 (Ck), 55.91 (Cm), 65.50 (Ca, Cb), 7.48 (Cc, Cd), 31.02 (Cl), 24.19 (C2–CH3), 22.59 (C4–CH3); MS (ESI): m/z: 363.25 $[M+H]^+$, 224, 211, 158, 144.

3.2.3.6 10-(3-[*N*-diethanolamino]propyl)-2,4-dimethylacridone (11e)

The procedure employed for **11a** was replicated with 1 g of **11,** 1.52 g of KI, 1.52 g of K_2CO_3 and 2.0 mL (0.35 mol) of *N,N*-diethanolamine. The oily residue was further purified by packing column chromatography with silica gel and free base obtained was dissolved in acetone and treated with ethereal HCl to generate stable HCl salt of **11e.**

Yield: 56%; mp: 193 ^{0}C; ^{1}H-NMR (500 MHz, [D_6]DMSO): 7.25–8.24 (m, 6H, Ar-H); 8.23 (d, 1H, H8, *J* = 8 Hz), 1.74-1.79 (s, 2-CH_3, 6H), 4.71 (s, 2H, He, Hf), 3.73 (m, 6H, Hc and Hd, Hk), 3.46 (m, 2H, Hm), 2.76 (m, 4H, Ha, Hb), 1.61–1.77 (m, 2H, Hl); ^{13}C-NMR (100 MHz, [D_6]DMSO): 178.27 (C9), 143.51 (C9', C8'), 143.69 (C10', C4'), 135.54 (C1), 131.76 (C7), 123.26 (C3), 127.91 (C5), 124.95 (C6), 123.79 (C8), 122.54 (C2), 119.35 (C4), 57.09 (Ck),

57.71 (Cm), 65.53 (Ca and Cb), 8.36 (Cc and Cd), 31.37 (Cl), 23.29 (C2–CH3), 22.67 (C4–CH3); MS (ESI): m/z: 394.78 $[M+H]^+$.

3.2.3.7 10-(3-*N*-[(β-hydroxyethyl)piperazino]propyl)-2,4-dimethylacridone (11f)

The procedure employed for **11a** was replicated with 1 g of **11,** 1.64 g of KI, 2.73 g of K_2CO_3 and 1.37 mL (0.35 mol) of β-hydroxyethyl piperazine. The oily residue was further purified by packing column chromatography with silica gel and free base obtained was dissolved in acetone and treated with ethereal HCl to generate stable HCl salt of **11f.**

Yield: 52%; mp: 223 ^{0}C; ^{1}H-NMR (500 MHz, [D_6]DMSO): 7.23-7.86 (m, 6H, Ar–H), 8.22 (d, 1H, Ar–H8, *J* = 4 Hz), 3.01–3.52 (m, 14H, Ha, Hb, Hc, Hd and He, Hk and Hm), 2.23 (t, 2H, Hl), 2.56- 3.01 (s, 6H, 2CH_3), 4.16 (s, 1H, OH); ^{13}C-NMR (100 MHz, [D_6]DMSO): 177.63 (C9), 145.05 (C9', C8'), 142.40 (C10', C4'), 135.07 (C1, C7), 128.12 (C3), 127.43 (C5), 124.32 (C6), 122.41 (C8), 119.56 (C2), 115.77 (C4), 59.15 (Cf), 56.74 (Ck, Cm), 49.40 (Ca, Cb), 42.69 (Cc, Cd), 29.55 (Ce), 27.83 (Cl), 25.54 (C2–CH_3), 23.48 (C4–CH_3); MS (ESI): m/z: 394.15 $[M+H]^+$.

3.2.3.8 10-(4-*N*-chlorobutyl)-2,4-dimethylacridone (12)

2,4-dimethylacridone (**10**) (1 g, 0.0021 mol) was dissolved in tetrahydrofuran (20 mL) and to it was added 6N KOH (25 mL) and tetrabutylammonium bromide (0.78 g) . The reaction mixture was continued stirring at room temperature for 30 min. To it 1-bromo-4-chlorobutane (0.24 mL, 0.0021 mol) was added dropwise and the reaction mixture was stirred for 24 hrs at RT. The solvent was evaporated under vacuum and the aqueous portion was extracted with $CHCl_3$ (3X20 mL). All the portions of organic layers were combined, washed with distilled water and dried (anhyd. Na_2SO_4) and the solvent was evaporated to give the crude product. The residue was further chromatographed with silica gel gave pure compound **12** as yellow solid.

Yield: 52 %; mp: 134 ^{0}C; ^{1}H-NMR (500 MHz, [D_6]DMSO): 7.0–7.6 (m, 6H, Ar–H, J = 8.3), 8.22 (d, 1H, H8, *J* = 8.2 Hz), 2.07 (m, 2H, Hl), 3.74-4.21 (t, 4H, Hk and Hn), 1.64–2.25 (m, 4H, Hl, Hm), 2.41-2.9 (s, 2CH_3); ^{13}C-NMR (100 MHz, [D_6]DMSO): 177.67 (C9), 144.45 (C9', C8'), 143.01 (C10', C4'), 132.59 (C1), 131.25 (C7), 129.07 (C3), 127.11 (C5), 124.45 (C6), 122.83

(C8), 116.11 (C2), 114.23 (C4), 54.84 (Ck), 51.47 (Cn), 25.28 (Cl), 24.26 (Cm) 21.53 (C2–CH3), 21.14 (C4–CH_3); MS (ESI): m/z: 313.52 $[M+H]^+$.

3.2.3.9 10-(4-*N*-morpholinobutyl)-2,4-dimethylacridone (12a)

10-(4-N-chlorobutyl)-2,4-dimethylacridone (**12**) (1 g, 0.0021 mol) was dissolved in ACN (30 mL) to which KI (1.55 g) was added along with K_2CO_3 (2.59 g) and refluxed for 30-40 min. Then morpholine (1.05 mL) was added to the reaction mixture and subjected to reflux for additional 20 hrs. The contents in the flask were cooled, diluted with distilled water and extracted with $CHCl_3$ (3X20 mL). All the portions of organic layers were combined, washed with distilled water and dried (anhyd. Na_2SO_4) and the solvent evaporated to give the product as oil. The oily residue was further purified by packing column chromatography with silica gel and free base obtained was dissolved in acetone and treated with ethereal HCl to generate stable HCl salt of **12a.**

Yield: 58%; mp: 148 ^{0}C; ^{1}H-NMR (500 MHz, [D_6]DMSO): 6.82– 7.75 (m, 6H, Ar–H, J = 4.2), 8.42 (d, 1H, H8, *J* = 4 Hz), 3.51–4.22 (m, 4H, Hc, Hd), 2.91–3.25 (m, 8H, Ha and Hb, Hk and Hn), 1.81–2.54 (m, 4H, Hm, Hl), 2.82 (s, 6H, 2 CH_3); ^{13}C-NMR (100 MHz, [D_6]DMSO): 179.55 (C9), 144.78 (C9', C8'), 142.35 (C10', C4'), 131.95 (C1), 130.97 (C7), 128.08 (C3), 127.27 (C5), 124.29 (C6), 122.23 (C8), 116.64 (C2), 114.66 (C4), 56.81 (Ck), 52.29 (Cn), 46.74 (Ca, Cb,) 62.39 (Cc, Cd), 25.48 (Cl, Cm) 23.07 (C2–CH3), 21.29 (C4–CH3); MS (ESI): m/z: 365.47 $[M+H]^+$.

3.2.3.10 10-(4-*N*-piperidinobutyl)-2,4-dimethylacridone (12b)

The procedure employed for **12a** was replicated with 1 g of **12,** 1.41 g of KI, 2.36 g of K_2CO_3 and 1.05 ml (0.35 mol) of piperidine. The oily residue was further purified by packing column chromatography with silica gel and free base obtained was dissolved in acetone and treated with ethereal HCl to generate stable HCl salt of **12b.**

Yield: 52%; mp: 162 ^{0}C; ^{1}H-NMR (500 MHz, [D_6]DMSO): 7.01– 7.64 (m, 6H, Ar–H, J = 8.3), 8.42 (d, 1H, H8, *J* = 8.4 Hz), 3.41–4.33 (m, 8H, Ha and Hb, Hk and Hn), 1.61–2.34 (m, 8H, Hc and Hd, Hl and Hm), 2.01 (m, 2H, He), 2.36-2.91 (s, 6H, 2 CH_3); ^{13}C-NMR (100 MHz, [D_6]DMSO): 177.15 (C9), 144.38 (C9', C8'), 142.07 (C10', C4'), 135.58 (C7), 128.81 (C1), 126.95 (C5), 122.04 (C6), 120.75 (C3), 119.92 (C8), 116.34 (C2), 114.71 (C4), 54.32 (Ck, Cn), 47.43 (Cl, Cm), 61.29 (Ca, Cb), 54.35 (Cc, Cd), 28.06 (Ce), 23.18 (C2–CH3), 21.34 (C4–CH3); MS (ESI): m/z: 363.65 $[M+H]^+$.

3.2.3.11 10-(4-*N*-methylpiperazino)butyl-2,4-dimethylacridone (12c)

The procedure employed for **12a** was replicated with 1 g of **12,** 1.43 g of KI, 2.38 g of K_2CO_3 and 1.0 mL (0.34 mol) of *N*-methylpiperazine. The oily residue was further purified by packing column chromatography with silica gel and free base obtained was dissolved in acetone and treated with ethereal HCl to generate stable HCl salt of **12c.**

Yield: 59%; mp: 183 ^{0}C; ^{1}H-NMR (500 MHz, [D_6]DMSO): 6.81– 7.62 (m, 6H, Ar–H, J = 8.2), 8.23 (d, 1H, *J* = 8 Hz), 4.31 (m, 8H, Ha, Hb Hc, Hd), 2.94 (m, 6H, He, Hk, Hn), 2.01–2.53 (m, 4H, Hl, Hm) 2.81- 3.14 (s, 6H, 2 CH3); ^{13}C-NMR (100 MHz, [D_6]DMSO): 179.56 (C9), 144.37 (C9', C8'), 142.04 (C10', C4'), 135.43 (C1), 131.16 (C7), 128.07 (C3), 127.09 (C5), 124.34 (C6), 122.88 (C8), 116.06 (C2), 114.14 (C4), 54.96 (Ck), 53.53 (Cn), 44.69 (Ca, Cb, Cc, Cd), 23.34 (Ce), 25.09 (Cl), 22.05 (Cm) 21.61 (C2–CH3), 21.09 (C4–CH3); MS (ESI): m/z: 378.22 $[M+H]^+$.

3.2.3.12 10-(4-[*N*-diethylamino]butyl)-2,4-dimethylacridone (12d)

The procedure employed for **12a** was replicated with 1 g of **12,** 1.57 g of KI, 2.62 g of K_2CO_3 and 1.3 mL (0.35 mol) of *N*,*N*-diethylamine. The oily residue was further purified by packing column chromatography with silica gel and free base obtained was dissolved in acetone and treated with ethereal HCl to generate stable HCl salt of **12d.**

Yield: 58%; mp: 172 ^{0}C; ^{1}H--NMR (500 MHz, [D_6]DMSO): 6.91–7.54 (m, 6H, Ar–H, J = 4.2), 8.26 (d, 1H, Ar–H8, *J* = 4.1 Hz), 4.21 (t, 2H, Hk), 3.06 (m, 6H, Ha, Hb and Hn), 2.03 (m, 4H, Hl, Hm) 2.21, 2.75 (s, 6H, 2 CH3); ^{13}C-NMR (100 MHz, [D_6]DMSO): 179.63 (C9), 144.96 (C9',

C8'), 142.39 (C10', C4'), 135.02 (C7), 127.34 (C1), 134.15 (C5), 128.13 (C6), 124.32 (C3), 122.32 (C8), 116.76 (C2), 114.77 (C4), 47.61 (Ck), 46.84 (Cn), 51.76 (Ca,s Cb), 9.84 (Cc, Cd), 25.59 (Cl, Cm), 23.14 (C2–CH_3), 22.59 (C4–CH_3); MS (ESI): m/z: 351.23 $[M+H]^+$.

3.2.3.13 10-(4-[*N*-diethanolamino]butyl)-2,4-dimethylacridone (12e)

The procedure employed for **12a** was replicated with 1 g of **12,** 1.8 g of KI, 2.8 g of K_2CO_3 and 1.2 mL (0.35 mol) of *N*-diethanolamine. The oily residue was further purified by packing column chromatography with silica gel and free base obtained was dissolved in acetone and treated with ethereal HCl to generate stable HCl salt of **12e.**

Yield: 52%; mp: 142 ^{0}C; ^{1}H-NMR (500 MHz, [D_6]DMSO): 7.23–8.45 (m, 6H, Ar-H); 8.25 (d, 1H, Ar–H8, *J* = 8 Hz), 1.75-1.79 (s, 2- CH3, 6H), 4.72 (s, 2H, He and Hf), 3.41 (m, 6H, Ha, Hb and Hn), 2.23 (m, 4H, Hl, Hm); ^{13}CNMR (100 MHz, [D_6]DMSO): 177.41 (C9), 141.57 (C9', C8'), 140.39 (C10', C4'), 135.61 (C7), 125.53 (C1), 134.12 (C5), 126.53 (C6), 124.37 (C3), 122.56 (C8), 117.79 (C2), 116.77 (C4), 48.61 (Ck), 44.22 (Cn), 54.75 (Ca,s Cb), 10.84 (Cc, Cd), 22.63 (Cl, Cm), 24.36 (C2–CH3), 20.81 (C4–CH3); MS (ESI): m/z: 383 $[M+H]^+$.

3.2.3.14 10-(4-*N*-[(β-hydroxyethyl)piperazino]butyl)-2,4-dimethylacridone (12f)

The procedure employed for **12a** was replicated with 1 g of **12,** 1.57 g of KI, 2.62 g of K_2CO_3 and 2.1 ml (0.35 mol) of β-hydroxyethyl piperazine. The oily residue was further purified by packing column chromatography with silica gel and free base obtained was dissolved in acetone and treated with ethereal HCl to generate stable HCl salt of **12f**.

Yield: 52%; mp: 142 ^{0}C; ^{1}H-NMR (500 MHz, [D_6]DMSO): 6.83–7.41 (m, 6H, Ar–H, J = 8.2), 8.16 (d, 1H, H8 *J* = 8.4 Hz), 3.72–4.15 (m, 9H, Hc, Hd, He, Hk), 2.91 (m, 2H, Hn), 1.71–1.94 (m, 4H, Hl and Hm), 2.15 (t, 2H, Hf), 2.62, (s, 6H, 2CH_3); ^{13}C-NMR (100 MHz, [D_6]DMSO): 177.54 (C9), 144.67 (C9', C8'), 142.13 (C10', C4'), 134.95 (C1), 135.08 (C7), 126.06 (C3), 125.52 (C5), 122.27 (C6), 119.52 (C8), 116.69 (C2), 114.64 (C4), 56.52 (Cf), 49.46 (Ce), 46.73 (Ck, Cn), 25.49 (Cc, Cd), 23.52 (Ca, Cb), 23.07 (Cl, Cm), 22.16 (C2–CH3), 21.67 (C4–CH_3); MS (ESI): m/z: 408.12 $[M+H]^+$.

3.3 Screening of acridone derivatives against Breast Cancer Cells:

Cytotoxic activity of acridones was determined from the sulforhodamine B (SRB) assay which measures the protein content of cells [54]. MCF-7 ells were grown in RPMI 1640 supplemented with 2 nM glutamine and fetal calf serum (10%) at 37 ^{0}C, CO_2 (5%) and air (95%). Logarithmically growing cells were collected by trypsinizing and washed with buffered saline, transferred to fresh cultured medium. Cell counting was done, transferred to 96-well culture plates and kept in incubator for 24 hrs to allow for attachment. Then the cells were observed under microscope and treated with varying concentrations of acridone derivatives. After 48 hrs, survival percentage of cells was determined by sulforhodamine B (SRB) binding assay. Cell survival was determined by quantifying the quantity of SRB from the measurements of absorbance at 540 nm of each well compared with the control wells. Control wells were treated with an equivalent amount of solvent i.e., ethanol used to prepare dilutions of test compounds is added. Each dilution of title compound was added in triplicate and IC_{50} values i.e., concentration of acridones required to inhibit protein synthesis was calculated by taking mean of triplicate readings.

3.4 Sensitization of resistant MCF-7/ADR cells by acridone derivatives

The drug resistant variant MCF-7/ADR cells were grown in RPMI 1640 supplemented with 2 nM glutamine and fetal calf serum (10%) at 37 ^{0}C, CO_2 (5%) and air (95%). Resistance to MCF7 cells was acquired by exposing to doxorubicin (MCF7/ADR cells). For consistent expression of MDR1 gene, MCF7/ADR cells were maintained in the presence of doxorubicin. Logarithmically growing cells were collected by trypsinizing and washed with buffered saline, transferred to fresh cultured medium. Cell counting was done, transferred to 96-well culture plates and kept in incubator for 24 hrs to allow for attachment. Then the cells were observed under microscope and treated with varying concentrations of acridone derivatives with varied concentrations of vinblastine (0-15 nM) for 48 hrs. After 48 hrs, survival percentage of cells was determined by sulforhodamine B (SRB) binding assay. Cell survival was determined by quantifying the SRB from the measurements of absorbance of each well compared with the control wells. MDR modulation activity of acridones in combination with vinblastine can be identified by calculating the IC_{50} values and comparing with IC_{50} of vinblastine alone. Control wells were treated with an equivalent amount of solvent i.e., ethanol used to prepare dilutions of test compounds is added. The reversal index of acridones (MRP1 antagonism score) was calculated as per the percentage

of surviving MCF-7/ADR cells in the absence of vinblastine/the percentage of surviving MCF-7/ADR cells in the presence of vinblastine.

3.5 Competition for [^{3}H]-Azidopine at active site of P-glycoprotein

3.5.1 Photoaffinity Labeling

Competition assay at the active site of P-gp was performed on membrane of KB-V1 cells. Resistance to KB-VI cells was acquired by exposing to vinblastine. For consistent expression of MDR1 gene, KB-VI cells were maintained in the presence of vinblastine. Cell membrane of cells was isolated from the cells of MDR variant KB-V1 as per protocol described [55]. Photolabelling of target protein P-gp was done by mixing with 100 nM of [^{3}H] azidopine with modulators **[11(a-f), 12(a-f)]** at their IC_{50} concentration in buffer with composition of sucrose (250 mM) and Tris HCl (10 mM) of pH 7.4 at 25 ^{0}C with final volume of 150 µL. Control was prepared without the addition of modulators. After mixing all the components, samples were kept for incubation in dark for 20 minutes. Then the samples were irradiated under germicidal UV light (GE Germicidal Lights, G30T8, 30 Watts) for 20 minutes.

3.5.2 SDS - PAGE and Autoradiography

Photolabeled proteins were separated under reduced conditions using buffer system by one dimensional 5-15% SDS-PAGE technique [56]. Later the gel was stained with coomassie blue and destained, soaked for 30 min in Amplify (Amersham Corp.) and kept for drying under vacuum at 75 ^{0}C. After drying, gels were developed by exposing to film at -70 ^{0}C for two to three days. Radioactive bands were scanned and quantified by integrating with chromatography recorder.

3.6 Computational Studies:

3.6.1 *In silico* prediciton of physicochemical properties

Physicochemical properties of the synthesized title compounds were calculated using QikProp module of Schrodinger software. The compounds were first drawn in 2D, prepared using Schrodinger's LigPrep module as per standard protocols. All the minimized structures were loaded into QikProp module and predicted the physicochemical properties.

3.6.2 Molecular docking

To identify the interactions of 2,4-disubstituted acridones with the P-gp, molecular docking studies were performed using Glide version 5.9, with default settings. The protein's X-ray crystallographic structure was retrieved from the protein data bank (PDB ID: 1MV5) and optimized by using OPLS2005 force field. All the synthesized 2,4-dimethylacridone derivatives in our laboratory were prepared and optimized using LigPrep 2.6 [57]. Receptor grid was generated at the active site and docking studies were performed by following the standard protocol [58]. Individual docked poses were inspected manually to observe the binding interactions of ligands with protein. All the molecular docking studies were performed on a Dell Inspiron laptop running Windows 7- 64 bit operating system and Intel i3 core processor 2.27 GHz, 3 GB RAM.

3.6.3 QSAR descriptors

Quantitative Structure Activity Relationship is one of the important and extensively used computational program to predict the anticancer activity and identify the relationship between the molecular descriptors and biological activity [59]. All the chemical structures of title compounds were drawn and minimized by standard protocol using Ligprep module of Schrodinger. After preparation of ligands, molecular descriptors were predicted by the Schrodinger's Qikprop module. Qikprop generates around 46 physically relevant descriptors to predict the drug likeness properties of the compounds. Selected descriptors of the acridone derivatives were used to build a QSAR model by one of the best method, Multiple Linear Regression (MLR) analysis [60]. Study was performed using Build QSAR software [51].

4 Conclusions:

In summary, title compounds N^{10}-substituted-2,4-dimethylacridone derivatives were syntheiszed by employing the principles of Ullmann condensation and phase transfer catalysis. Antiproliferative activity was evaluated against both sensitive and resistant cancer cell lines and SAR studies were reported. Present study illustrated that 2,4-dimethylacridones were potential modulators of MDR mediated through P-gp. The structural features of these compounds included

acridone which is tricyclic and hydrophobic with an electron-donating methyl groups at 2nd and 4th positions with an alkyl side chain of length three or four and ended with tertiary amines. The influence of propyl and butyl side chain between the acridone ring and the tertiary amine was examined. Butyl chain was found to be optimum for the biological activity. Selectivity of acridones with butyl side chain was observed towards resistant cancer cells and interestingly acridone with secondary amine β-hydroxyethyl piperazine was found active among the title compounds. The results of the present investigation identified the factors contributing N^{10}-substituted-2,4-dimethylacridone derivatives for cytotoxicity were length of alkyl side chain and chemical nature of secondary amine attached. Title compounds with tertiary amines containing hydroxyl group as substituent have enhanced cytotoxicity in both cancer sensitive and resistant cells. QSAR study too has identified the significant molecular descriptors which contribute the cytotoxicity. Best regression equation was obtained with significant correlation between predicted and observed cytotoxicity values by multiple linear regression (MLR) analysis. Hence, it is worthwhile to consider 2,4-dimethylacridone as lead and can be exploited for further design and development of the safe and potent MDR modulators.

Acknowledgement:

The authors thank Department of Science & Technology, Government of India, Project No. SR/FT/LS- 186/2009 for funding. MCY also thanks Shri Vile Parle Kelavani Mandal for necessary support, Mr. R. Raghu and Schrodinger team for providing academic evaluation license to carry out the molecular docking studies.

Conflict of interest:

The authors confirm that this article content has no conflicts of interest.

References:

[1] M.M. Gottesman, T. Fojo, T, S.E. Bates, Multidrug resistance in cancer: role of ATP-dependent transporters, Nat. Rev. Cancer. 2 (2002) 48-58.

[2] G. Cholewinski, K. Dzierzbicka, M.M. Koodziejczyk, Natural and synthetic acridines/acridones as antitumor agents: their biological activities and methods of synthesis, Pharmacol. Rep. 63 (2011) 305-336.

[3] Q. Wu, Z. Yang, Y. Nie, Y. Shi, D. Fan, Multi-drug resistance in cancer chemotherapeutics: mechanisms and lab approaches. Cancer Lett. 347 (2014) 159-166.

[4] Y. Yan, M. Bjornmalm, F. Caruso, Particle carriers for combating multidrug resistant cancer, ACS Nano. 7 (2013) 9512-9517.

[5] M.M. Gottesman, Mechanisms of Cancer Drug Resistance, Annu. Rev. Med. 53 (2002) 615-627.

[6] T. Ozben, Mechanisms and strategies to overcome multidrug resistance in cancer, FEBS Lett. 580 (2006) 2903-2909.

[7] M. Saraswathy, S. Gong, Different strategies to overcome multidrug resistance in cancer, Biotechnol. Adv. 31 (2013) 1397-1407.

[8] G.K. Hughes, F.N. Lahey, J.R. Price, L.J. Webb, Alkaloids of the Australian Rutaceae. Nature. 162 (1948) 223–224.

[9] G.H. Svoboda, G.A. Poore, P.J. Simpson, G.B. Boder, Alkaloids of Acronychia Baueri Schott I. Isolation of the alkaloids and a study of the antitumor and other biological properties of acronycine, J. Pharm. Sci. 55 (1966) 758–768.

[10] M. Demeunynck, F. Charmantray, A. Martelli, Interest of acridine derivatives in the anticancer chemotherapy, Curr. Pharm. Des. 7 (2001) 1703–1724.

[11] R.T. Dorr, J.D. Liddil, D.D. Von Hoff, M. Soble, C.K. Osborne, Antitumor activity and murine pharmacokinetics of parenteral acronycine. Cancer Res. 15 (1989) 340–344.

[12] M. Kozurkova, P. Kristian, D. Sabolova, I. Danihel, Acridine Isothiocyanates: Chemistry and Biology. in: Kristian, P. (Eds.), Lambert Academic Press, 2014, pp. 150– 161.

[13] J. Plsikova, L. Janovec, J. Koval, J. Ungvarsky, J. Mikes, R. Jendzelovsky, P. Fedorocko, J. Imrich, P. Kristian, J. Kasparkova, V. Brabec, M. Kozurkova, 3,6- Bis(3-alkylguanidino)acridines as DNA-intercalating antitumor agents, Eur. J. Med. Chem. 57 (2012) 283–295.

[14] J. Plsíkova, J. Stepankova, J. Kasparkova, V. Brabec, M. Backor, M. Kozurkova, Lichen secondary metabolites as DNA-interacting agents, Toxicol. In Vitro. 28 (2014) 182–186.

[15] M. Malachowska-Ugarte, G. Cholewinski, K. Dzierzbicka, P. Trzonkowski, Synthesis and biological activity of novel mycophenolic acid conjugates containing nitro-acridine/acridone derivatives, Eur. J. Med. Chem. 54 (2012) 197-201.

[16] T.L. Su, K.A. Watanabe, Anticancer acridone alkaloids, in: B.S. Atta-ur-Rahman, F.Z. Basha, F.Z., (Eds), Studies in Natural Products Chemistry, Elsevier, Amsterdam, 1993, pp. 347-382.

[17] K.F. Bastow, M. Itoigawa, Antiproliferative actions of 7-substituted 1,3-dihydroxyacridones; possible involvement of DNA topoisomerase II and protein kinase C as biochemical targets, Bioorg. Med. Chem. 2 (1994) 1403-1411.

[18] B. Zhang, K. Chen, N. Wang, C. Gao, Q. Sun, L. Li, Y. Chen, C. Tan, H. Liu, Y. Jiang, Molecular design, synthesis and biological research of novel pyridyl acridones as potent DNA-binding and apoptosis-inducing agents, Eur. J. Med. Chem. 93 (2015) 214-226.

[19] Y.C. Mayur, Designing of Drug Molecules for Reversing P-glycoprotein (P-gp) Mediated Drug Resistance in Cancer Cells in: B.S. Atta-ur-Rahman, Iqbal Choudhary, M., (Eds.), Frontiers in anti-cancer drug discovery, Bentham Science Publishers, Amsterdam, 2015, pp. 157-198.

[20] T.W. Loo, D.M. Clarke, The Transmembrane Domains of the Human Multidrug Resistance P-glycoprotein Are Sufficient to Mediate Drug Binding and Trafficking to the Cell Surface, J. Biol. Chem. 274 (1999) 24759-24765.

[21] G.E. Jara, D.M. Vera, A.B. Pierini, Binding of modulators to mouse and human multidrug resistance P-glycoprotein. A computational study, J. Mol. Graph. Model. 46 (2013) 10-21.

[22] V.V.S. Rajendra Prasad, G. Deepak Reddy, D. Appaji, G.J. Peters, Y.C. Mayur, Chemosensitizing acridones: in vitro calmodulin dependent cAMP phosphodiesterase inhibition, docking, pharmacophore modeling and 3D QSAR studies, J. Mol. Graph. Model. 40 (2013) 116-124.

[23] A. Wallstab, M. Koester, M. Bohme, D. Keppler, Selective inhibition of MDR1 P-glycoprotein-mediated transport by the acridone carboxamide derivative GG918, Br. J. Cancer 79 (1999) 1053–1060.

[24] S.V. Ambudkar, C. Kimchi-Sarfaty, Z.E. Sauna, M.M. Gottesman, P-glycoprotein: from genomics to mechanism, Oncogene. 22 (2003) 7468-7485.

[25] E. Tseng, E.A. Scott-Ramsay, M.E. Morris, Dietary organic isothiocyanates are cytotoxic in human breast cancer MCF-7 and mammary epithelial MCF-12A cell lines, Exp. Biol. Med. (Maywood). 229 (2004) 835-842.

[26] J. Budworth, R. Davies, J. Malkhandi, T.W. Gant, D.R. Ferry, A. Gescher, Comparison of staurosporine and four analogues: their effects on growth, rhodamine 123 retention and binding to P-glycoprotein in multidrug-resistant MCF-7/Adr cells, Br. J. Cancer. 73 (1996) 1063-1068.

[27] J.P. Gillet, Sudhir Varma, M.M. Gottesman, The clinical relevance of cancer cell lines, J. Natl. Cancer Inst. 105 (2013) 452-458.

[28] M.M. Cornwell, A.R. Safa, R.L. Felsted, M.M. Gottesman, I. Pastan, Membrane vesicles from multidrug-resistant human cancer cells contain a specific 150- to 170-kDa protein detected by photoaffinity labelling, Proc. Natl. Acad. Sci. 83 (1986) 3847-3850.

[29] D.W. Shen, C. Cardarelli, J. Hwang, M. Cornwell, N. Richert, S. Ishii, I. Pastan, M.M. Gottesman, Multiple drug-resistant human KB carcinoma cells independently selected for high-level resistance to colchicine, adriamycin, or vinblastine show changes in expression of specific proteins, J. Biol. Chem. 261 (1986) 7762-7770.

[30] I.B. Roninson, J.E. Chin, K.G. Choi, P. Gros, D.E. Housman, A. Fojo, D.W. Shen, M.M. Gottesman, I. Pastan, Isolation of human mdr DNA sequences amplified in multidrug-resistant KB carcinoma cells, Proc. Natl. Acad. Sci. U S A. 83 (1986) 4538-4542.

[31] H.M. Kim, G.T. Oh, D.H. Hong, M.S. Kim, J.S. Kang, S.M. Park, S.B. Han, MDR-1 gene expression is a minor factor in determining the multidrug resistance phenotype of MCF7/ADR and KB-VI cells, FEBS Lett. 412 (1997) 201-206.

[32] E.P. Bruggemann, S.J. Currier, M.M. Gottesman, I. Pastan, Characterization of the azidopine and vinblastine binding site of P-glycoprotein, J. Biol. Chem. 267 (1992) 21020-21026.

[33] E. Rutkowska, K. Pajak, K. Jóźwiak, Lipophilicity methods of determination and its role in medicinal chemistry, Acta Pol. Pharm. 70 (2013) 3-18.

[34] B.C. Baguley, G.J. Finlay, Derivatives of amsacrine: determinants required for high activity against Lewis lung carcinoma, J. Natl. Cancer Inst. 80 (1988) 195-199.

[35] M. Maliepaard, N.J. de Mol, L.H. Janssen, W. van der Neut, W. Verboom, D.N. Reinhoudt, Role of lipophilicity in the in vitro antitumor activity of a series of new mitosene compounds, Anticancer Drug Des. 7 (1992) 415-425.

[36] Z. Mazerska, E. Augustin, J. Dziegielewski, M.W. Chołody, J. Konopa, QSAR of acridines, III. Structure–activity relationship for antitumor imidazoacridinones and intercorrelations between *in vivo* and *in vitro* tests, Anticancer Drug Des. 11 (1996) 73-88.

[37] I. Facchetti, M. Grandi, P. Cucchi, C. Geroni, S. Penco, A. Vigevani, Influence of lipophilicity of anthracyclines in LoVo and LoVo/Dx human cell lines, Anticancer Drug Des. 6 (1991) 385-397.

[38] D.J. Adams, L.R. Morgan, Tumor Physiology and Charge Dynamics of Anticancer Drugs: Implications for Camptothecin-based Drug Development, Curr. Med. Chem. 18 (2011) 1367–1372.

[39] R. Prankerd, Critical compilation of pKa values for pharmaceutical substances, Profiles Drug Subst. Excip. Relat. Methodol. 33 (2007) 1-33.

[40] B.P. Mahoney, N. Raghunand, B. Baggett, R.J. Gillies, Tumor acidity, ion trapping and chemotherapeutics I. Acid pH affects the distribution of chemotherapeutic agents *in vitro*, Biochem. Pharmacol. 66 (2003) 1207–1218.

[41] N. Raghunand, R.J. Gillies, pH and drug resistance in tumors, Drug Resist. Updat. 3 (2000) 39–47.

[42] G. Sosnovsky, P. Bell, In the search for new anticancer drugs. 29. A study on the correlation of lipophilicities, ionization constants and anticancer activities of aminoxyl labeled tepa congeners, Life Sci. 62 (1998) 639-648.

[43] C. Liao, M. C. Nicklaus, Comparison of nine programs predicting pKa values of pharmaceutical substances, J. Chem. Inf. Model. 49 (2009) 2801-2812.

[44] B. Testa, L.B. Kier, The concept of molecular structure in Structure-Activity Relationship studies and drug design, Med. Res. Rev. 11 (1991) 35-48.

[45] G.K. Ravindra, G. Achaiah, G.N. Sastry, Molecular modeling studies of phenoxy-pyrimidinyl imidazoles as p38 kinase inhibitors using QSAR and docking, Eur. J. Med. Chem. 43 (2008) 830–838.

[46] S. Janardhan, P. Srivani, G.N. Sastry, 2D and 3D quantitative structureactivity relationship studies on a series of bis-pyridinium compounds as choline kinase inhibitors, QSAR Combi. Sci. 25 (2006) 860–872.

[47] S.H. Kumar, A comparative QSPR study of alkanes with the help of computational chemistry, Bull. Kor. Chem. Soc. 30 (2009) 67–76.

[48] M.R. De Jonge, L.M. Koymans, H.M. Vinkers, F.F. Daeyaert, J. Heeres, P.J. Lewi, P.A. Janssen, Structure based activity prediction of HIV-1 reverse transcriptase inhibitors, J. Med. Chem. 4 (2005) 2176–2183.

[49] L. Miguet, A. Zervosen, T. Gerards, F.A. Pasha, A. Luxen, M. Disteche-Nguyen, A. Thomas, Discovery of new inhibitors of resistant streptococcus pneumoniae penicillin binding protein (PBP) 2x by structure-based virtual screening, J. Med. Chem. 52 (2010) 5926–5936.

[50] S.Y. Liao, C. Chen, L. Qian, Y. Shen, K.C. Zheng, QSAR studies and molecular design of phenanthrene-based tylophorine derivatives with anticancer activity, QSAR Combi. Sci. 27 (2008) 280–288.

[51] D.B. De Oliveira, A.C. Gaudio, BuildQSAR: A new computer program for QSAR analysis, Quant. Struct.-Act. Relat. 19 (2000) 599-601.

[52] M.H. Bohari, H.K. Srivastava, G.N. Sastry, Analogue-based approaches in anti-cancer compound modelling: the relevance of QSAR models, Org. Med. Chem. Lett.1 (2011) 3.

[53] I.P. Beletskaya, A.V. Cheprakov, Copper in cross-coupling reactions The post-Ullmann chemistry, Coordin. Chem. Rev. 248 (2004) 2337–2364.

[54] Y.P. Keepers, P.E. Pizao, G.J. Peters, J. van Ark-Otte, B. Winograd, H.M. Pinedo, Comparison of the sulforhodamine B protein and tetrazolium (MTT) assays for in vitro chemosensitivity testing, Eur. J. Cancer. 27 (1991) 897-900.

[55] G.A. Altenberg, M. Subramanyam, L. Reuss, Muscarinic stimulation of gallbladder epithelium. III. Antagonism of cAMP-mediated effects, Am. J. Physiol. 267 (1994) C1196-1202.

[56] U.K. Laemmli, Cleavage of structural proteins during the assembly of the head of bacteriophage T4, Nature. 277 (1970) 680-685.

[57] Lig prep ver. 2.6, Schrödinger LLC, New York, NY (USA), 2010.

[58] Glide ver. 5.9, Schrödinger LLC, New York, NY (USA), 2010.

[59] J. Portugal, Evaluation of molecular descriptors for antitumor drugs with respect to noncovalent binding to DNA and antiproliferative activity, BMC Pharmacol. 9 (2009) 11.

[60] N.R. Draper, H. Smith, Applied Regression Analysis, (Eds.), John Wiley & Sons, New York, 1981, 153-174.

Highlights

- A new series of 2,4-dimethylacridones with propyl and butyl side chain containing terminally substituted tertiary amines have been synthesized
- Compounds were evaluated against drug sensitive and resistant cell lines
- Compounds **12e** and **12f** have exhibited good cytotoxicity profile against both MCF7 and MCF7/ADR cell lines
- Molecular Docking studies too supported the experimental observations
- QSAR equation was derived using BuildQSAR programme to identify the molecular descriptors